DOI: 10.1002/anie.201001180

Crystallization

In-Situ Monitoring of the Formation of Crystalline Solids

*Nicole Pienack and Wolfgang Bensch**

Keywords:
crystallization · in-situ monitoring · solid-state chemistry · spectroscopic methods · X-ray diffraction techniques

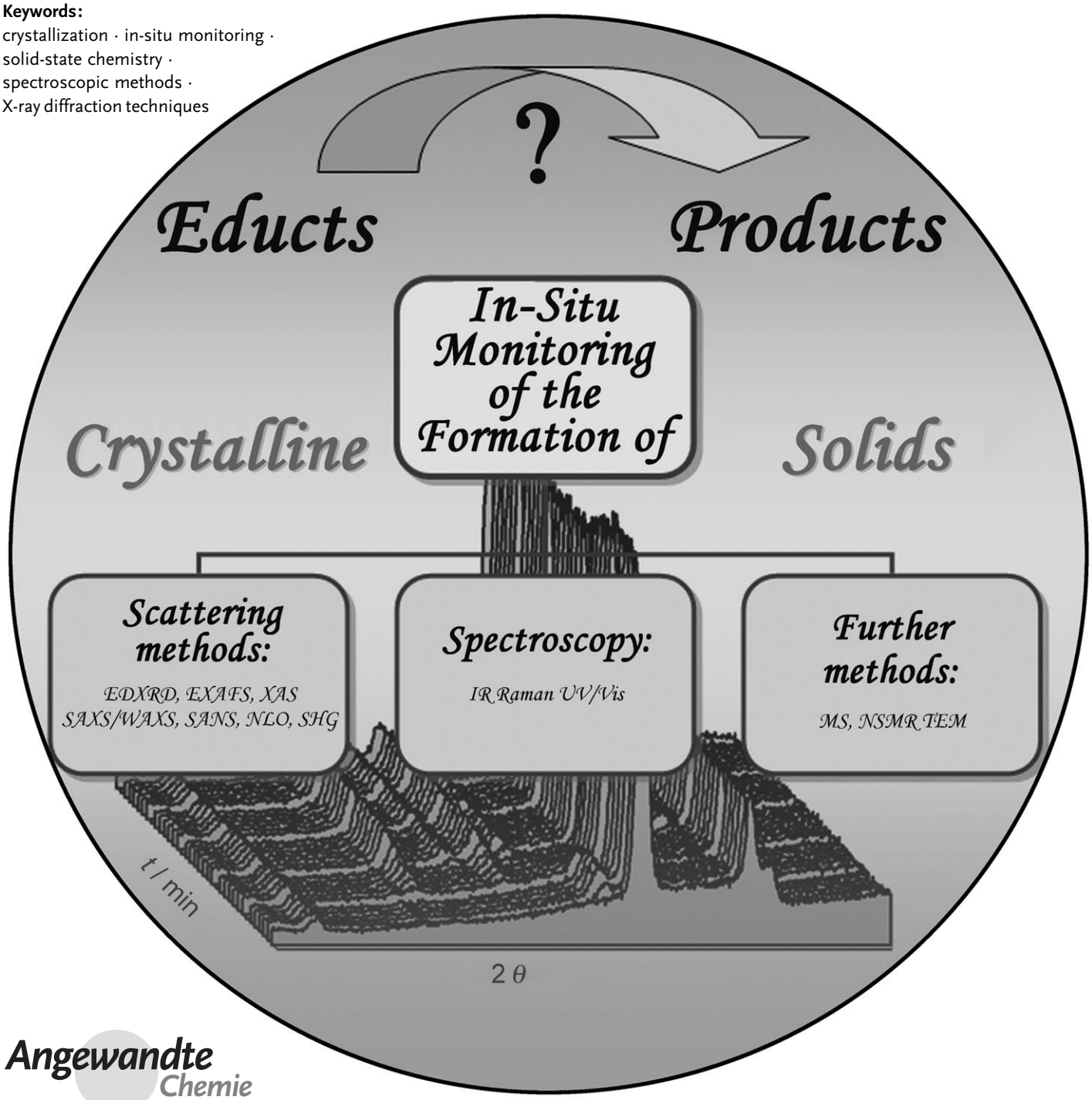

The processes occurring during the early stages of the formation of crystalline solids are not well understood thus preventing the rational synthesis of new solids. The investigation of the structure-forming processes is an enormous challenge for both analytical and theoretical methods because very small particles or aggregates with different chemical composition and different sizes must be probed, both before and during nucleation. Furthermore, these precursors are present in a complex and dynamic equilibrium. This Review gives a survey of the in-situ methods available for the study of the early stages of crystallization of solids and how they can help in the synthesis of metastable polymorphs, of transient intermediates, and/or precursors displaying new or improved properties. Examples of actual research demonstrate the necessity and potentials but also the limitations of in-situ monitoring of the formation of crystalline solids.

From the Contents

1. Introduction

The main goal of the research in the chemical sciences is the synthesis of new compounds. The challenges for the future, for example, in areas such as, energy conversion (e.g. thermoelectrics), energy storage (lithium batteries, hydrogen storage), energy harvesting (solar energy, H_2 production from water), energy efficiency (e.g. light emitting diodes (LEDs)), data recording, data processing, and data storage (e.g. phase change materials in DVDs) require the development of new materials which display new and/or improved properties. Hence, there is a broad and increasing interest for a rational synthesis of such materials. Especially in solid-state chemistry the preparation of new materials and the investigation of structure–property relationships are the focus of research interests. But the prediction of synthesis products is at best limited, and usually more or less impossible. Crystalline solids are one of the most important classes of compounds for the development of materials. But an understanding of the preparation of such materials is still at the early stages of development. Crystalline solids are characterized by a tight structure–property relationship based on pronounced cooperative phenomena, that is, the crystal structure and the chemical composition determine the resulting chemical and physical properties. Such properties are "generated" during the development of the crystal structure. Owing to the direct relationship between the different properties and the crystal structure of a solid, the synthetic accessibility of potential crystalline solids, including metastable phases of different combinations of chemical elements, plays a key role in the development of new materials with interesting properties.

To date, the essential atomistic knowledge of the structure-forming processes during the 'birth' of a crystalline solid is missing. These fundamental steps include the pre-organization in homogeneous media, the demixing, the aggregation and nucleation and subsequent crystallization. But without information about these initial events the directed synthesis of new stable or metastable solids is very difficult. The basic relationships are well known but a control over these individual steps is (still) not possible.

The formation of a crystalline solid from solution should serve as an example to highlight the problems investigating the formation of crystalline solids under real conditions. If supersaturation is reached, the system is characterized by a high free energy which may be reduced by the formation of a solid phase of the dissolved substance. The formation of the solid phase leads to a reduction of the chemical potential (volume potential) of the system, which can be regarded as the driving force for seed (nucleus) building. At this stage of the reaction small agglomerates consisting of about 100 atoms are formed which are in equilibrium with the solution. The formation of the solid phase leads to the formation of a surface for which the surface energy must be generated. Summarizing briefly, the total chemical potential of the system at this stage is the sum of the volume (energy reduction) and the surface potential (energy enhancement). Plotting the change of these potentials against the radius of the nucleus, a maximum of the total potential will be reached at a distinct value for the radius which is called the critical radius r_c. During nucleation only those nuclei with a radius larger than r_c will survive whereas nuclei with $r < r_c$ will be dissolved. During reaction progress these supercritical nuclei grow through incorporation of dissolved species and finally reach sizes of macroscopic crystals. Afterwards, further processes, such as Ostwald ripening or re-crystallization in a more stable phase according to Ostwald's rule, may occur. A detailed presentation of the nucleation-crystallization theory is beyond the scope of this Review and the reader should consult literature such as the recently published Review.[1]

The essential problems of experimentally probing the nucleation of a solid out of a solution in real systems are obvious: the subcritical nuclei are in the nanometer range or smaller, the lifetime of the nuclei is very short, and they can

[*] Dr. N. Pienack, Prof. Dr. W. Bensch
Christian-Albrechts-Universität zu Kiel
Institut für Anorganische Chemie
Max-Eyth-Strasse 2, 24118 Kiel (Germany)
Fax: (+49) 880-1520
E-mail: wbensch@ac.uni-kiel.de

move freely in the reaction volume, reducing the chance to monitor these nuclei within the experimentally accessible volume section. In addition, the interface between solid and solvent moves very fast. A possible approach to investigate the fundamental steps of crystal formation more in detail is the usage of colloidal model systems. Monodisperse colloids with particle sizes between about 100 nm and a few μm may be regarded as "atoms". Owing to the large size of these "atoms" the necessary experimental effort is relatively low as such colloids can be investigated by, for example, optical microscopy because the distance between the "atoms" is in the range of visible light. Furthermore, the individual processes in such systems are slow, different types of interactions can be realized easily—except covalent bonding interactions—and theoretical simulation of the processes in such systems is straightforward.[2,3] But it is questionable whether the results obtained with such model systems can be transferred to real reaction systems.

The synthesis of a thermodynamically stable crystalline solid is sometimes not easy but in most cases the problems occurring can be solved. It is more difficult to rationally prepare a metastable crystalline phase. To "enforce" a desired crystal structure for a given chemical composition, control over the first steps during the formation of the structure must be realized. It is still a big challenge to steer a synthesis towards a distinct local free-enthalpy minimum. In recent years, several theoretical publications demonstrated that the phase space of viable crystalline solids is surprisingly large. But only a few of these predicted solids could be synthesized to date.[4]

It can be assumed that new materials may also be obtained away from the thermodynamic equilibrium by applying kinetically controlled synthesis methods, that is, thermodynamically metastable crystalline solids can only be prepared under non-equilibrium conditions. Such conditions are obtained by decreasing synthesis temperature, shorter reaction times, or quenching of reactions. There are several synthesis methods available allowing the preparation of metastable crystalline solids. These include solvothermal conditions, heterogeneous nucleation, thin-film couples, desolvatation, topotactic or epitactic reactions in the bulk phase, deposition of reactants at very low temperature and subsequent slow warming, metathesis reactions, directed thermal decomposition, rapid expansion of supercritical solutions (RESS), mechanochemical methods (tribochemistry, high-energy ball milling), achievement of very high supersaturation by addition of an anti-solvent, or utilization of different energies of nucleation barriers. The large potential of these methods is constantly being demonstrated.

In spite of the large variety of synthesis methods, it is very often not possible to decide what synthetic approach or strategy is suitable for the preparation of a desired solid compound, or what reaction parameters must be altered to optimize the preparation of a new crystalline solid. For a certain compound theoretical calculations and energetic considerations may lead to the exclusion of unsuitable synthesis conditions, however, the synthetic work cannot be substituted by calculations.

In-situ methods are appropriate to acquire the missing knowledge about the mechanisms occurring under reaction conditions. By applying such methods important questions can be answered concerning polymorphism, conversion of solids, the occurrence of short-living crystalline intermediates and/or precursors during chemical reactions. But such in-situ experiments must not be restricted to the solid itself and it is absolutely necessary to probe the most important parameters of the mother phase (solvent, amorphous solid, etc.) by applying the appropriate methods.

Crystalline intermediate phases are often metastable and may have different properties than the thermodynamically stable products. The potentially interesting properties of still unknown but viable polymorphs cannot be used currently because the structure-forming processes are not understood. It is highly likely that the so-called "disappeared" polymorphs mentioned in the literature can be ascribed to the restricted predictability of syntheses.[5] Once a metastable modification of a compound could be synthesized, a second more-stable modification may occur which may be formed accidentally. As a consequence of the occurrence of the more stable form, the metastable polymorph cannot be prepared again or transforms into the stable form within a short time. A very prominent example for this event is the active substance Ritonavir in an important AIDS drug (trade name Norvir, Abbott Laboratories).

With respect to the type of in-situ investigations, those that are most powerful allow reactions to be monitored under real conditions without disturbing the reacting systems. But it should be kept in mind that several in-situ experiments can only be performed at special research centers which will be discussed in Section 2. If the experimental boundary conditions are appropriate for solving a distinct problem, in-situ experiments can also be undertaken with normal laboratory

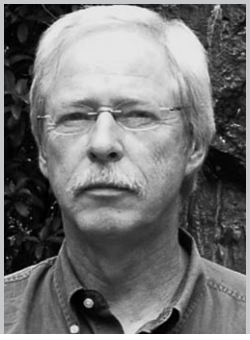

Wolfgang Bensch studied chemistry at the LMU in Munich. After finishing his PhD in 1983 he was a PostDoc at the University of Zürich. He then joined Siemens for 3 years. He finished his habilitation 1993 in Frankfurt (Johann-Wolfgang-Goethe Universität) and since 1997 he has been professor for inorganic solid-state chemistry at the Christian-Albrechts-Universität, Kiel (Germany).

Nicole Pienack studied chemistry at the Christian-Albrechts-Universität, Kiel (Germany). In 2008 she finished her PhD thesis on solvothermal syntheses of modified transition-metal containing thiostannates. She is now member of the scientific staff in the Institute for Inorganic Chemistry at the same university.

facilities. In principal, chemical reactions can be quenched during the reaction. But it is impossible to be sure that the true reaction state is quenched and captured with such ex-situ experiments.

Before reactions are investigated with in-situ methods it is necessary to consider what information should be acquired and what method is appropriate to gain this information. In addition, the prerequisites that must be fulfilled to utilize a specific technique should be verify. The choice of the analytical instruments depends on different questions, such as whether atomic, local, or long-range-order information alone is satisfactory or whether such information should be acquired in parallel. Further important questions should be clarified in advance such as if the experimental method should be atom specific, how much material is required for the investigation, and if the investigation provide time and/or site specific information. For instance, if solvothermal reactions or syntheses with alkali metals are to be investigated under in-situ conditions, special reaction cells are required. Such in-situ instruments must often be constructed and adapted to the experimental conditions, for example, high temperatures, aggressive media, high pressures. Often this is an iterative process until the optimal instrument is at hand. It is clear that a universal cell cannot be realized because it is impossible to design an instrument that allows investigations of different reactions with very different basic experimental conditions. Indeed in-situ instruments can be constructed in a flexible way, such as our cell allowing in-situ energy-dispersive X-ray diffraction (EDXRD) investigations under normal and solvothermal conditions or intercalation reactions at DESY (Deutsches Elektronen Synchrotron).[6–8]

A complete discussion of all aspects of in-situ investigations is beyond the scope of this Review, and therefore we focus on selected aspects of the methods. Ex-situ experiments involving quenching or interrupting reactions after distinct reaction times and subsequent characterization of the products will not be considered herein. Furthermore, nanoparticles displaying a size-dependent polymorphism will also not be discussed. In addition, we restrict the presentation to those analytical techniques and methods where the formation of crystalline solids is the focus of the research work. We are aware that many interesting in-situ experiments have been performed on, for example, solid catalysts, biomolecules, mesoporous materials, pharmaceuticals. But in most of these studies the investigation of the formation mechanisms of a crystalline solid was not the focus of the experiments. Therefore the reader should consult appropriate Review articles.[9]

Herein we first present an overview about the most important in-situ methods and we proceed in presenting selected examples demonstrating the performance of the methods. We restrict the Review to those methods which are not widely established for the investigation of the formation of solids. In addition we only present some basic principles of the methods and for a deeper understanding references are given. Theoretical basics of well established methods, such as infrared spectroscopy, Raman spectroscopy, or nuclear magnetic resonance (NMR) spectroscopy will not be presented and we restrict the presentation on selected examples that demonstrate the potential of these methods for monitoring the formation of solids.

2. Selected In-Situ Methods

The formation of crystalline solids can be monitored with different methods, and X-ray as well as neutron scattering techniques are very promising. But other techniques are also of interest, such as IR and Raman spectroscopy which allow acquisition of deep insights into reactions occurring under real synthesis conditions. In many cases a combination of different analytical methods is necessary because one method alone cannot deliver all desired information. In Table 1 some suitable methods are summarized some of which are presented in more detail in this Section. In Section 3 selected examples are discussed demonstrating the performance and the limitations of the methods.

Table 1: List of suitable in-situ methods.

Methods
Scattering methods:
Energy dispersive X-ray diffraction (EDXRD)
X-ray absorption spectroscopy (XAS)
Small-angle scattering
... with X-rays (SAXS)
... with neutrons (SANS)
Wide-angle X-ray scattering (WAXS)
Neutron diffraction (ND)
Spectroscopy:
Vibrational spectroscopy
... Infrared spectroscopy (IR)
... Raman spectroscopy
Mass spectrometry (MS):
Electrospray-Ionization-MS (ESI-MS)
Further techniques:
Transmission electron microscopy (TEM)
NMR spectroscopy

2.1. In-Situ Scattering Techniques

The large potential of in-situ scattering techniques was recognized at the beginning of 1990s, and since then they were applied in a larger number of investigations.[10] Mainly solid catalysts and/or micro- and mesoporous materials were the focus of these studies.[11] The combination of complementary methods, such as energy-dispersive X-ray scattering (EDXRD) and X-ray absorption spectroscopy (XAS), is very powerful.[7,12] Other characterization techniques, such as in-situ small-angle scattering (SAS) are particularly established in polymer chemistry, material sciences, and colloid chemistry.[9d,13]

2.1.1. Energy-Dispersive X-ray Diffraction (EDXRD)

Scattering experiments, such as energy dispersive X-ray diffraction is a very suitable method to follow the formation of crystalline or partially crystalline solids under in-situ conditions. During chemical reactions, crystalline intermedi-

ates or precursors can be easily detected and under certain conditions these solids can be identified. Furthermore, the development of such intermediates/precursors can be monitored during reaction progress. An enormous advantage of in-situ EDXRD is that the influence of different reaction parameters on the reaction progress and the product formation can be investigated without repetition of the synthesis.[11a] For instance, spectra can be collected during heating and/or cooling of the reaction slurry yielding information about the dissolution rate of solid starting materials or transformation of a solid phase. To achieve a high time resolution and a good signal-to-noise ratio, in-situ EDXRD experiments are mainly performed with synchrotron radiation. A distinct energy range of the white synchrotron beam is selected to guarantee that in a polycrystalline sample with statistical orientation of the crystallites a wavelength or photon energy for Bragg scattering/diffraction is always present. Simultaneously detecting the generated X-ray fluorescence lines of the elements in the reaction mixture may yield further information about the reaction progress. Besides the simultaneous detection of many Bragg reflections, the high intensity of the synchrotron radiation leads to a good time resolution. Using laboratory X-ray sources the collection of one powder pattern often requires several hours whereas diffractograms can be collected within minutes using synchrotron radiation, and in special cases within seconds. In addition the intensity of synchrotron radiation is high enough to penetrate the walls of reaction vessels, such as stainless steel autoclaves allowing experiments under high pressure, for example, which is not possible with standard laboratory conditions. A disadvantage of in-situ EDXRD is the relatively low resolution of the spectra which is problematic for crystalline materials with reflections lying close together. Nevertheless, considering the boundary conditions, detailed insights into the reaction progress and the crystallization kinetics can be achieved. Plotting the change of the reaction progress against the reaction time the so-called Avrami-Exponent can be determined allowing some conclusions about the mechanism of crystallization.

In-situ X-ray scattering experiments have mainly been used to monitor the formation of technologically and industrially relevant materials, such as zeolites or zeotype materials. Since 1992 the formation of such crystalline solids was relatively often studied such as, the formation of sodalite,[10b] zeolite A,[10b,14] Co^{2+}/Zn^{2+}-exchanged zeolite A,[15] the hydrothermal conversion of zeolites,[16] or the crystallization of gallo-, alumino-, and zincophosphates.[11a,c,14a,b,17] In addition, in-situ EDXRD studies were undertaken to monitor the hydrothermal formation of thio- or selenometalates[7,18] and of other compounds.[8a–c,19] The in-situ EDXRD approach is also suitable to study intercalation, ion-exchange reactions of different host materials,[20] and other chemical reactions;[12c,21] see also the Review in Ref. [22].

2.1.2. *X-Ray Absorption Spectroscopy (XAS)*

Extended X-ray absorption fine structure (EXAFS) and X-ray absorption near-edge spectroscopy (XANES) or near-edge absorption fine structure (NEXAFS) are suitable methods to probe the local environment of atoms for a range of up to about 1 nm. The breakthrough of X-ray absorption fine structure in the 1980s was made possible by the availability of synchrotron radiation and the theoretical background for evaluation of the spectra.[23]

The principal of EXAFS is based on the absorption of X-rays by inner electrons of an atom (absorber atom) and the registration of the change of their absorption coefficient as a function of the energy of the X-rays. The method is element specific and the local environment even of neighboring elements in the periodic table can be distinguished. If a substance is irradiated with X-rays with varying energy, an electron of the absorber atom is excited at a distinct energy (threshold energy) and is promoted into the continuum. This absorption event is accompanied by a steep increase of the absorption coefficient. The threshold energy depends on the chemical state of the absorber atom, and referencing of the energy value against the elemental state allows an estimation of the formal oxidation state of the absorber atom and the covalency of the chemical bond to the neighboring atoms. In a simple picture, the emitted photoelectron can be treated as a wave which is scattered by the neighboring atoms (see Figure 1). The outgoing photoelectron wave of the absorber interferes with the waves backscattered by the neighboring atoms leading to a modulation of the absorption coefficient. The modulations occur in the spectrum as oscillations above the absorption edge and due to destructive and constructive interferences minima and maxima occur. The modulations contain the information about the type, number, and the distance to the neighboring atoms.[23]

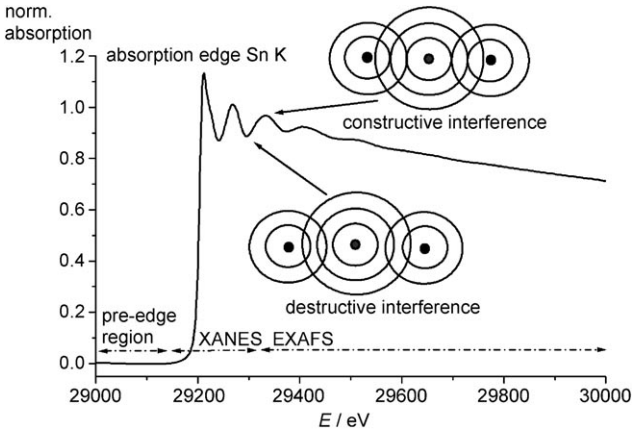

Figure 1. X-ray absorption spectrum of a thiostannate solution recorded at beamline X1 (Hasylab, DESY) at the Sn K-edge (29.2 keV) in transmission mode. The constructive and destructive interference outgoing from the absorber are displayed. The different regions of the spectrum are also indicated (pre-edge, XANES, and EXAFS).

The EXAFS region of a spectrum extends from about 50 to 1000 eV above the absorption edge of the corresponding absorber atom, while XANES covers the energetic region from the absorption edge to the beginning of the EXAFS (near edge region; Figure 1). In the XANES region the incoming photon energy is not large enough to promote the

electron directly to the continuum so that the photoelectron first occupies empty electronic states (bound states) or energetically low-lying empty states near the continuum.

Because the photoelectron is scattered several times by the neighboring atoms, an exact quantum-mechanical description is difficult,[23f] and the XANES spectra are often used as a fingerprint region. The comparison of the spectrum with those of known compounds allows conclusions to be drawn concerning the type and number of neighboring atoms. In the EXAFS region the kinetic energy of the emitted electron is large and only single scattering events occur, and consequently the theoretical description is less complex than for the XANES region. In many cases pronounced features are observed in the pre-edge region, which are caused by dipole-allowed transitions of the photoelectron. Such features give direct evidences for the geometric environment around the absorber atom because such electronic transitions are only dipole allowed for non-centrosymmetric coordination polyhedra. The spectrum of an absorber in a tetrahedral environment can display a very intense pre-edge peak whereas for an octahedral environment such a feature is often not observed. The information cannot be directly extracted from the spectra and after processing of the raw data the structure information is obtained applying the EXAFS equation which establishes a relationship between structural parameters and modulation frequencies. Despite XAFS being an element specific method, the spectra contain only an averaged value for all the atoms of the same element. Especially for atoms adopting different local environments, the structure cannot be extracted without a suitable structural model. In-situ EXAFS experiments are often combined with complementary methods, such as X-ray scattering and small-angle X-ray scattering (see Section 3).

The EXAFS and XANES experiments can be performed on crystalline, amorphous, liquid, or gaseous substances. Both methods probe the short-range order around an atom and clearly these techniques are most suitable to probe the early stages of nuclei formation, that is, at stages long before the formation of the crystalline solid. In the sub-critical nuclei, the most important structural information is restricted to the direct-neighbor atoms. Therefore, the time- and temperature-dependent changes of the local environment during a chemical reaction can be monitored. But without special instrumentations EXAFS is a slow method and even using the quick-EXAFS mode the accumulation of a suitable spectrum requires seconds depending on the substance and the sample environment. Only with energy-dispersive EXAFS is the collection of spectra in the hundred millisecond time regime possible.[24] We want to note that ultrafast EXAFS and XANES experiments in the picosecond or femtosecond time regimes, respectively, can be performed using highly advanced instrumentations. But such experiments are predominantly applied for pump–probe experiments to monitor dynamic phenomena.[25] In addition, most synchrotron sources supply only a certain energy range and depending on the scientific problem in-situ experiments must be performed on different sources. It is very important in planning such experiments to consider the sample environment, because when X-rays have to travel long distances through the reaction mixture pronounced absorption effects occur, especially for soft X-rays, and the resulting spectrum exhibits a poor signal-to-noise ratio complicating or even preventing an evaluation.

2.1.3. *Small-Angle X-Ray Scattering (SAXS), Wide-Angle X-Ray Scattering (WAXS), and Anomalous Small-Angle X-Ray Scattering (ASAXS)*

Small-angle X-ray scattering (SAXS) is applied for the analysis of nanoscale structures to determine the size and shape of particles as well as their interactions. In contrast to the classical X-ray diffraction on lattice planes (Bragg condition for scattering), in a SAXS experiment the interaction between X-rays and objects of different shapes with sizes between 1 and >100 nm is probed.[26] The sample is irradiated with monochromatic X-rays and the elastic interaction of the photons with the electrons of the sample generates secondary waves which are summed to the total structure amplitude. The scattering curves are typically measured only at very small scattering angles. The secondary waves are characterized by an identical frequency but owing to the different path lengths the phases may be different (Figure 2). In the simplest case, isotropic spherical particles without any long-range ordering are distributed homogeneously in a matrix whereby the matrix can be viewed as homogeneous medium with its own electron density. This situation corresponds to spherical particles in solution or inhomogeneities in a solid.

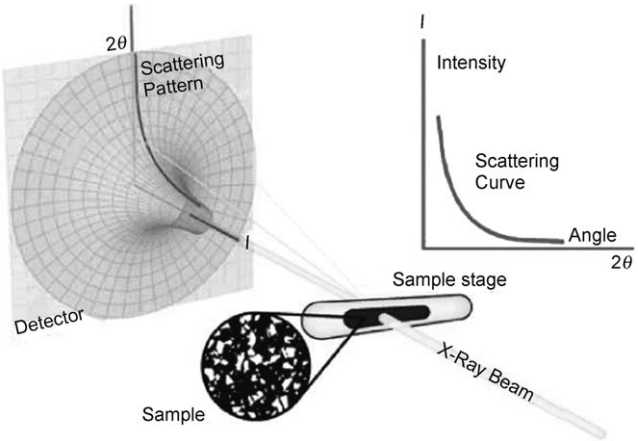

Figure 2. Schematic representation of the principle of small-angle X-ray scattering.[27]

In the SAXS curves, different regions of the intensity versus scattering-vector curve are distinguished (Figure 3). Directly above the backscattering region, the curve follows the Guinier region with particle sizes $qR \ll 1$ (q is the scattering vector, R = particle size). Above the Guinier region the scattering curve follows a power law (Porod region) and from the exponent the shape of the particle can be deduced.

The evaluation of SAXS scattering curves yields information about the size, shape, orientation, and surface of particles

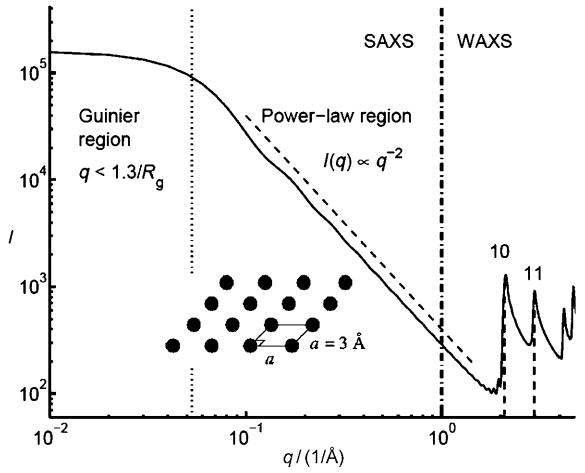

Figure 3. The different regions in the intensity versus scattering curve in a SAXS experiment.[28]

(Figure 4), and SAXS is therefore suitable for in-situ monitoring of the formation of solids at the very early stages. The SAXS experiments are performed with monochromatic X-rays preventing any conclusion being drawn about the chemical composition or the assembly of the particles, that is, for complex systems the assignment of contributions of individual components to the total scattering curve is not possible. Such complex situations are found for example, in core–shell particles or nanoscopic precipitations in alloys.

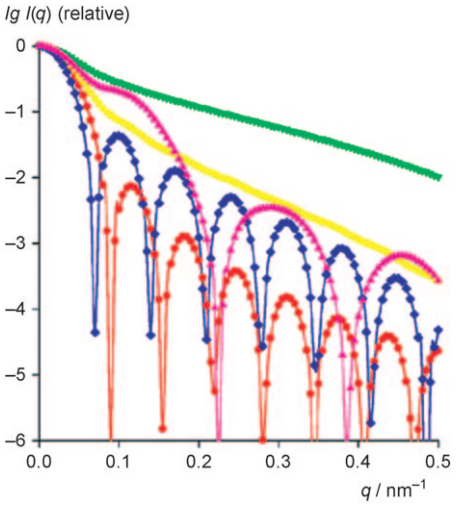

Figure 4. Simulated SAXS curves for different particle shapes. ● red: spheres; ▼ green: rods; ■ yellow: flat plates; ◆ blue: hollow spheres; ▲ violet: dumbbells. Reprinted from Ref. [29] with permission of the IOP Publishing.

To achieve an assignment to distinct chemical elements in a particle, a deconvolution of the individual contributions to the total scattering curve is necessary. Such a partition is achieved utilizing the anomalous dispersion (anomalous small-angle X-ray scattering, ASAXS; see for example, Ref. [30]). The atomic form factor of a chemical element differs significantly near the absorption edge and this difference is more pronounced for heavier elements. In so-called contrast experiments the SAXS curves are measured near the absorption edge and far away from this edge. The curves are then subtracted giving a separate scattering curve for the element that was measured at the absorption edge (contrast separation). For a two-component system at least three scattering curves must be measured for a confident interpretation of the data. The number of experimental stations for ASAXS investigations is limited (roughly one dozen around the world) and the expenditure on equipment is extraordinary high because a very high beam stability is required. SAXS or ASAXS are often used to investigate substances such as nanoparticles, gels, polymers, liquid crystals, micro-emulsions, biomolecules.[13b–d,19a–e] The greatly increased research interest in recent years in the field of nanoscale materials has initiated a rapid development of both the instrumentation and of suitable measurement cells for in-situ small-angle scattering experiments.[31]

With typical laboratory X-ray sources no suitable time resolution can be reached and measurement times up to a few hours are required to collect patterns that can be interpreted with confidence. Using well-focused synchrotron radiation (diameter a few 10 μm) gives a significant reduction of the measurement time and good scattering curves may be obtained within minutes. In combination with special experimental set-ups, such as stop-flow or jet-stream cells, SAXS curves can be recorded within microseconds. The high intensity of the synchrotron radiation also allows the investigation of reactions in extreme sample environments, for example, under hydrothermal or high-temperature conditions.

The information obtained with SAXS/ASAXS about the particle formation is often not sufficient because a full characterization and the combination with other analytical methods is required. In cases where information about the crystalline structure of a material should be acquired, X-ray reflections at higher scattering angles can be collected simultaneously using WAXS which is a method similar to conventional X-ray diffraction. Combination of SAXS, ASAXS, and WAXS in one experiment yields information about the structural organization of a solid on different lengths scales. The formation of Al-Zr-Si ceramics was monitored with temperature-resolved in-situ SAXS,[32] as was the hydrothermal crystallization of a clay mineral.[33] The crystallization of silicalite-1 (pure ZSM-5) under different synthesis conditions was intensively studied by in-situ SAXS experiments.[34]

2.1.4. *Small-Angle Neutron Scattering (SANS) and Neutron Diffraction (ND)*

The most important advantage of neutrons over X-rays is the low absorption of neutrons by most elements. This property allows the in-situ investigation of samples in special environments, such as autoclaves, cryostats, or pressure cells.[19a] Because the scattering process occurs at the atomic nucleus, light elements, such as hydrogen, can be detected. In addition, the scattering power of neighboring elements and

also of isotopes, for example, hydrogen and deuterium, differ significantly. A pronounced contrast enhancement can be achieved by deuteration of a hydrogen-containing substance. The high incoherent scattering background of H-containing samples can be used to monitor the removal of hydrogen during a chemical reaction. Because collimation of neutrons is more or less impossible, the sample volume must be relatively large. Compared to the intensity of X-rays, the neutron flux is very low even at the best neutron sources. As a consequence fast reactions and processes cannot be probed. In-situ neutron scattering experiments were applied, for example, to investigate solid–solid conversions, dehydration reactions, decomposition reactions, phase transitions, intercalation reactions,[35] the hydrothermal formation of zeolites and layered silicates,[36] the temperature-dependent crystallization of ZrO_2 from Zr hydroxides,[37] and the pressure-dependent formation of metal hydrides.[38] Analogous to SAXS, small-angle neutron scattering (SANS) probes particles in the size region from about 1 to 100 nm. The advantage of SANS over SAXS is that the intensity contrast between particles and the medium (solvent) can be drastically increased by deuteration allowing determination of the chemical composition of the particles. For instance, the contrast method was applied to study the ageing and crystallization processes during the synthesis of ZSM-5 and silicalite.[39]

2.2. In-Situ Spectroscopy

In addition to the scattering techniques, other methods, such as in-situ IR, ATR-IR (attenuated total reflection IR), and Raman spectroscopy are suitable to acquire mechanistic information about the formation of crystalline solids and a better understanding of the processes occurring during the reactions.[40] For a comprehensive understanding of the different steps in the crystallization of a solid from solution the knowledge of the species in solution and their concentration is of fundamental importance. Only if this information is available can a relationship between the crystallized solid and the molecular building units in solution be established.

Some selected spectroscopic methods are briefly discussed below. Vibrational spectroscopy is a very suitable technique to monitor reactions of organic solids, the transition of organic polymorphs, and to identify species in solution, because small changes of the force field caused by structural alterations can be easily detected. But without a special instrumentation IR, ATR-IR, and Raman spectroscopy are relatively slow methods and are more appropriate for studies in the minute time scale. The particular strength of ATR-IR spectroscopy is the determination of the concentration of dissolved species, which is of special relevance for the formation of solids from solution. Raman microscopy combined with a CCD camera or special reaction-cell design allows collection of good spectra on a second time scale with resolutions in the μm^2 region. Reactions of thin films can be monitored applying confocal Raman spectroscopy reaching a depth resolution of a few μm. In cases where a high time resolution is not required the smallest amounts of substances (nanogram) can be probed. In the near IR region, Raman spectra are less complex than IR spectra and the Raman modes are better resolved simplifying significantly quantification of the species present. In addition, Raman scattering in aqueous solution is low while IR radiation is heavily absorbed by OH groups. A serious problem of Raman spectroscopy is undesired fluorescence which disturbs the Raman signals or even hides the modes. Generally the intensity of the fluorescence decreases with increasing excitation wavelength. On the other hand, the signal intensity is inverse proportional to λ^4 and in the short-wavelength region resonances have a low intensity. If Raman studies are performed in solution only noisy spectra with low information content can be measured when the solubility of a solid is low. But besides detection of small structural changes or distortions, varying hydration or protonation states, changes of charge and defect distribution, alterations of the surface, disordered building units, and short-range order/disorder can be monitored, which is not possible with X-ray scattering. This performance of Raman spectroscopy is widely used in the pharmaceutical industry for in-line control,[41] for example, the quantitative analysis and determination of concentration of active substances,[42] of the amorphous proportion,[43] quantitative determination of the amount of different polymorphs and their transformation as function of time.[44] For example, in combination with in-situ X-ray scattering at a synchrotron facility, different transformations of solids under non-ambient conditions could be studied with reasonable good time resolution.[45]

To date, most in-situ Raman spectroscopy studies were performed on pharmaceutically relevant compounds. Some exceptions are presented below. Using a special cell the formation of zeolite X under hydrothermal conditions could be studied with in-situ UV-Raman spectroscopy with a time resolution in the minute range.[46] In-situ Raman investigations of the crystallization of MeAPO-34 demonstrated that complex interactions between the metal ion and the conformation of the organic structure-directing molecule are most important, whereas for the formation of ALPO-5 only the conformation of the "template" is relevant.[47] In a temperature-resolved in-situ Raman study of the crystallization of $Ba_2Ti_2O_5$ from a precursor glass, the formation of the high-symmetric α-phase could be detected first, followed by the crystallization of the low-symmetric β-modification at elevated temperatures. The crystallization of the α-modification is initiated by homogeneous nucleation and three-dimensional diffusion-limited growth, while the β-phase crystallizes through heterogeneous nucleation.[48] A detailed picture about the crystallization of a $Bi_{4-x}La_xTa_3O_{12}$ film could also be obtained applying temperature-resolved in-situ Raman spectroscopy.[49]

A drawback of IR spectroscopy is the strong absorption by solvents so that the crystallization of solids can only be followed using a very thin cuvette. This drawback can be overcome applying ATR-IR spectroscopy. The IR radiation is transmitted through an IR transparent crystal with a large refraction index so that the IR beam experiences several total reflections within the crystal. The crystal (e.g. diamond) and the sample to be probed are in direct optical contact (Figure 5). A small part of the IR radiation emerges from the ATR crystal (evanescent wave) penetrating the sample up

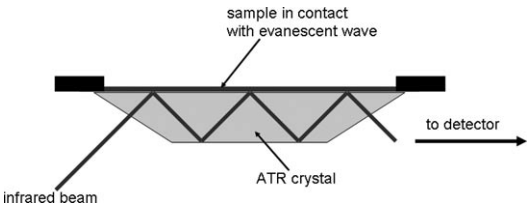

Figure 5. The principal of ATR-IR spectroscopy (adapted from Ref. [50]).

to a certain depth (0.5–5 μm). The more often the IR radiation is reflected within the ATR crystal, the more often information about the sample is obtained and the signal-to-noise ratio is improved and the measurement time is reduced.

The main applications of in-situ ATR-FT-IR spectroscopy are in pharmaceutical chemistry. With this technique the solubility of polymorphs is investigated (time and temperature resolved) as well as supersaturation phenomena.[51] However, time and spatial resolutions are low and fast crystallization cannot be probed with this method. Note that based on the quantum confinement effects, such as changes in the optical band gap, the alteration of the size of particles can be monitored with UV/Vis spectroscopy.

2.3. In-Situ Mass Spectrometry

For advanced analytical applications of mass spectrometry, different measurement principles have been developed which differ mainly with respect to the ionization process and the detection of intact macro- and biomolecules.[52] However, real in-situ conditions can only be achieved by direct coupling of the mass spectrometer to tube or so-called batch reactors. For example, applying this set-up, the time- and temperature-dependent alterations of oligomers in silicate solutions before crystallization could be studied for example, for ZSM-5, ZSM-11, silicalite-1, silicalite-2, and germanium-containing zeolites.[53,54]

2.4. In-Situ Transmission Electron Microscopy

For monitoring reactions with atomic resolution, transmission electron microscopy (TEM) is a very suitable technique.[55] In principal, local information at reacting interfaces of solids can be obtained. The combination of TEM with other techniques including, nano-element-analytics (energy dispersive X-ray (EDX)), energy-filtering (EFTEM), electron energy-loss spectroscopy (EELS, ELNES) and atomic number contrasting, selected-area electron diffraction (SAED), and tomography enables the reacting interfaces as well as the change of the chemical state of the reacting elements to be monitored with atomic resolution. Hence TEM/HRTEM is an attractive method to investigate the early stages of nucleation. Because TEM/HRTEM experiments can only be performed under ultra-high-vacuum conditions the kinds of reaction systems that can be investigated is considerable restricted. In addition the substances must be stable against the intense electron beam and a movement of the position of the sample during in-situ heating experiments must be strictly prevented. Even high-energy electrons can penetrate only very thin samples (a few 100 nm) and therefore sample preparation is elaborate. Hence it is not surprising that only very few real in-situ TEM/HRTEM experiments have been reported.[56] An example is the crystallization of $LiFePO_4$ from the amorphous state. At the beginning, a transient crystalline intermediate could be identified which is transformed into the ordered $LiFePO_4$ structure by several phase transitions of intermediary formed crystalline phases.[56e]

2.5. In-Situ NMR Spectroscopy[40b,57]

NMR spectroscopy has become a powerful analytical tool for in-situ investigations, this is due to the development of sample containers for experiments at elevated temperatures or under hydrothermal conditions, the establishment of techniques such as magic-angle spinning (MAS), cross polarization MAS (CP-MAS) as well as the development of new pulse sequences. NMR spectroscopy probes the local environment of atoms and the changes of the environment during crystallization can be investigated.[57b] To achieve acceptable time resolution, suitable NMR nuclei with good sensitivity must be present in the sample. But even if a compound or solution contains such atoms the acquisition of a spectrum requires several minutes. Compounds with suitable nuclei for NMR spectroscopy are for example, zeolites and many zeotype materials, such as alumino, gallo, or silico-alumino phosphates (ALPO, GAPO, SAPO). The crystallization of such materials from gels is relatively slow so that species in solution as well as their structural changes can be followed with in-situ NMR spectroscopy. Examples for such experiments are the studies of crystallization of SAPO-34,[58] zeolite A,[59] ALPO-4,[60] ULM and MIL,[61] or boron-containing ZSM-5.[62] Because different species in solution are in equilibrium, an unambiguous identification can often only be achieved by accompanying theoretical calculations. CP-MAS-NMR spectroscopy allows differentiation between the species in solution and the solid in the solvent. For example, the transition of α-glycine into the more stable γ-modification could be studied using this technique for the first time.[63]

2.6. Combination of Methods

Every single method discussed in this Section records the formation of solids with different length, time, spatial, elemental, and concentration resolution. But it is also necessary to acquire and evaluate information about the mother phases, such as liquids or amorphous precursors, in an appropriate manner and not only about the crystalline solid. Hence it is clear that a single method can only supply a piece of the jigsaw puzzle and only the combination of different in-situ methods allows extensive conclusions about the formation of a crystalline solid. Therefore, it is not surprising that often different in-situ methods are combined to attain a

comprehensive picture (see for example, Ref. [19a, 64]). In addition, accompanying ex-situ characterizations must be performed to guarantee that the formation of the desired product was studied. The interpretation of results obtained with in-situ methods is more convincing if they are supported by theoretical modeling, simulation and/or calculations performed at different levels. During the last few years significant progress was made in these areas of theory. For the theoretical research it is important to distinguish between the structure prediction for planning the synthesis (potential target structures), the approaches for the computational structure determination, and the theoretical investigation of the mechanisms of nucleation processes. In the area of synthesis planning, potential structure candidates could be identified using global energy optimization.[4b] The determination, the prediction, and the understanding of structures of crystalline solids can be achieved through exploration of the energy landscape of chemical systems.[4c,65] The performance of this concept was impressively documented in a number of publications.[66] During the last few years further theoretical concepts were applied to synthesis planning. For instance, high-pressure phases were identified by systematic exploration of the energy landscape using ab-initio approaches.[67] New crystalline solids with hitherto unknown structures can be predicted by simulating the interconnection of secondary building units.[68] Further theoretical studies deal with the prediction of crystalline polymorphic solids, atomistic mechanisms of the phase separation of simple model systems, the prediction of crystal structures,[69] the molecular dynamic (MD) simulation of nucleation rates,[70] or the MD simulation of activated processes[71] (see also Ref. [72]). A comprehensive representation of the different theoretical methods and approaches to simulate nucleation mechanisms of crystalline solids is presented by Anwar and Zahn in this Issue.[73]

3. Selected Examples of In-Situ Experiments

In this Section selected examples are presented to demonstrate the potential of in-situ investigations to give an impression of which systems can be treated and how to proceed.

3.1. Investigation of the Formation of Crystalline Solids from Solution

Several technologically important solids (zeolites and analogous compounds) are synthesized under solvo- or hydrothermal conditions. But this synthetic approach is also applied to synthesizing, for example, chalcogenidometalates,[6,7,19g,74] polyoxometallates,[75] or oxides.[76] Solvothermal syntheses are heterogeneous reactions and a large number of parameters such as, temperature, time, solvent, pH value, or concentration influence product formation in a way that is not well understood.[77] In the overwhelming number of cases the products were obtained rather by accident then by planning or design. A detailed insight into the reactions is required for a more directed/rational synthesis planning. Such insights may be obtained using in-situ investigations, such as time-resolved energy dispersive X-ray diffraction which allows probing the reactions under real conditions. For an evaluation of the crystallization kinetics often a few hundred, and in special cases, a few thousand patterns must be quantitatively analyzed. It is also very important to perform experiments more than one time to demonstrate reproducibility of the results.[10b,11b,20b–c,36,78]

3.1.1. Crystallization of Thiometallates

Our group investigated the formation of thioantimonates with composition $Mn_2Sb_2S_5{\cdot}L$ (L = amine) applying in-situ EDXRD. The compounds can be obtained as phase-pure materials in high yield from elemental Mn, Sb, S in aqueous amine solutions at $T = 100$–$180\,^{\circ}C$. Suitable amines include, methylamine (MA), 1,3-diaminopropane (DAP), *N*-methyl-diaminopropane (MDAP), or diethylenetriamine (DIEN). Therefore, this group of compounds is very suitable to study the influence of the amine on the formation mechanisms and the crystallization kinetics. Using L = DAP the time until the first reflections appear in the spectrum (induction period) strongly depends on the reaction temperature. Reducing the synthesis temperature below 105 °C a crystalline precursor appears first, followed by a crystalline intermediate. The intermediate compound and the desired product are in close relation because the intensity of the reflections of the intermediate decline as soon as reflections of the product appears. About the nature of this relationship can only be speculated. The intermediate compound could not be isolated in quenching experiments. Analogous observations, that metastable intermediates could not be isolated were reported by several other authors.[11a,12a] Applying L = MDAP, product growth is faster than for L = DAP, and using L = DIEN the fastest growth is observed. However, crystallization starts much later owing to a longer incubation time. In contrast to L = DAP, no crystalline intermediates or precursors could be detected using L = MDAP. Product formation for L = DIEN is totally different. At the beginning of the reaction, a crystalline precursor appears which could be isolated using quenching experiments. Chemical analysis revealed that the precursor contained only Mn, S, and the amine. After a few minutes, the precursor disappeared and reflections of the first short-living crystalline intermediate could be observed, followed by the appearance of a second intermediate which was more stable than the first one. After this sequence of formation of crystalline precursor/intermediates the product $Mn_2Sb_2S_5{\cdot}$DIEN started to crystallize. These observations suggest that different consecutive and/or parallel mechanisms occur at the beginning of the reaction which are significantly influenced by the amine used. Results of syntheses with L = MDAP indicate that at lower temperatures nucleation is the rate-limiting step while at elevated temperatures diffusion-controlled reactions dominate. After a longer induction period, the formation of $Mn_2Sb_2S_5{\cdot}$DIEN proceeds by diffusion control. In competitive syntheses using amine mixtures only $Mn_2Sb_2S_5{\cdot}$DIEN could be identified as final product, that is, this compound is thermodynamically more stable than the other compounds. Performing solvothermal reactions with

crystalline $Mn_2Sb_2S_5$·DAP and $Mn_2Sb_2S_5$·MDAP as starting materials in a DIEN solution a complete conversion into the DIEN containing product is observed. Presumably the conversion proceeds by partial dissolution of the educts followed by immediate crystallization of $Mn_2Sb_2S_5$·DIEN.

The investigations demonstrate that the crystallization of nearly isostructural compounds may follow different mechanisms and the amine supplied determines the mechanism of product formation. Because in-situ EDXRD can only detect the crystalline phases, information about species in the solution and composition or the structure(s) of the critical nuclei is missing. Such information may be acquired using complementary methods such as EXAFS and/or SAXS.

3.1.2. *Investigation of the Formation of Zeotype Zinc Phosphates*

The structures of zeolites and zeolite-like materials are determined by the synthesis conditions and the presence of structure directing molecules, such as amines or organic ammonium salts. The integration of heteroelements such as zinc and the substitution of the silicate by phosphate species leads to new open-framework structures which exhibit different properties compared to pure Si or Si/Al containing materials. The formation mechanisms of such phosphate containing zeotype materials are mainly unexplored. The complex nature of the hydrothermal formation of a zeotype zinc phosphate was demonstrated with in-situ EDXRD experiments.[11b] The syntheses were performed with piperazinium phosphate (PIP-P) and ZnO in acidic solution. After dissolution of the starting materials a well-known zinc phosphate **I** with chain structure is detected at room temperature. At about 163 °C additional reflections of a second, unknown phase **II** occur. A few minutes after reaching the reaction temperature of 180 °C the reflections of **I** and **II**, as well as those of non-dissolved ZnO are substituted continuously by reflections of two other zinc phosphates **III** and **IV**. On increasing the concentration of PIP-P, first phase **I** appears which decomposes within a very short time period and the zinc phosphate **V** crystallizes. The detailed analysis of the results suggests that the transformation of **I** into **V** is a solvent-mediated process and not a solid-to-solid transformation.

3.1.3. *Metastable Modifications of $NaNbO_3$*

Oxides with perowskite structure are often utilized in actuators, relaxors, piezo- and pyroelectric devices. Doped $NaNbO_3$ derivatives display piezoelectric properties and are of special interest as lead-free alternative materials to substitute lead zirconium titanates (PZT).[79] The compound $NaNbO_3$ is polymorphic and the different variants crystallize in related perowskite-type structures.

Very recently $NaNbO_3$ could be prepared under hydrothermal conditions (240 °C, Nb_2O_5 (**1**), 1 M NaOH, 3 h) in the metastable ilmenite modification. In-situ EDXRD experiments performed with two different NaOH concentrations yield a detailed picture of the reaction pathway to the final product. Using a 1.5 M NaOH solution only $NaNbO_3$ with the perowskite structure (**P**) could be obtained after 1 h (Figure 6). During the reaction, first $Na_7(H_3O)Nb_6O_{19}$·14 H_2O (**2**) was formed, followed by crystallization of $Na_2Nb_2O_6$·*n* H_2O (**3**). Similar phases were isolated and

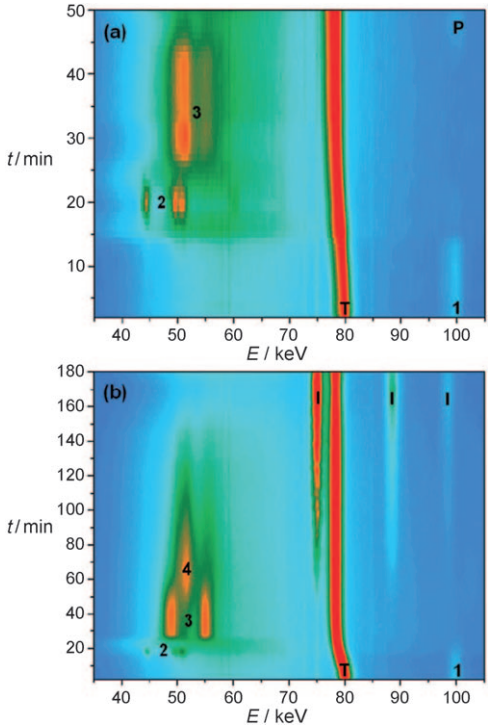

Figure 6. In-situ EDXRD patterns of the hydrothermal formation of $NaNbO_3$. Explanation of the numbers and letters is given in the main text.[19j] Reproduced with permission from the Royal Society of Chemistry (RSC).

identified using quenching experiments.[80] On decreasing the NaOH concentration to 1 M, only the ilmenite modification crystallized after 3 h reaction time. Again the first compound to appear was $Na_7(H_3O)Nb_6O_{19}$·14 H_2O (**2**) followed by crystallization of $Na_2Nb_2O_6$·*n* H_2O (**3**). But in contrast to the synthesis with the higher NaOH concentration an unknown crystalline intermediate **4** was observed before formation of $NaNbO_3$ with the ilmenite-type (**I**) structure.[19j]

3.1.4. *Phase Conversion of Cobalt Hydroxides*

In the examples presented above the crystallization of the solids was only monitored with in-situ X-ray scattering. But with this technique no information about the nature and number of particles which are formed during and after crystallization can be acquired. Such information can be obtained simultaneously combining in-situ EDXRD with SAXS and WAXS. Applying this combination of techniques, the phase conversion of different α-Co^{II} hydroxides into the β-modification could be clarified.[19e] The layered cobalt hydroxides crystallize in different modifications and the α-form is of more interest for electrochemical applications than the β-polymorph. The structure of the α-form consists of positively charged $Co(OH)_{2-x}$ layers with charge compensating anions located in the interlayer spaces. In contrast, the β-

form contains neutral layers. The α-$Co(OH)_{2-x}Y_x$-phases (Y = anion) spontaneously converts into the β-form when they come in contact with alkali cations, and little is known about the pathway of the conversion reactions. The conversion of $Co(OH)_{1.4}(NCO)_{0.6}\cdot 0.6\,H_2O$ (**5**) into β-$Co(OH)_2$ (**8**; Figure 7) is diffusion controlled while the conversion of

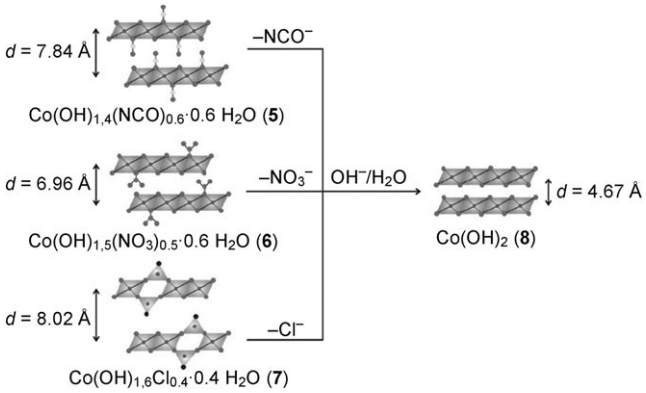

Figure 7. The phase-conversion reactions of different Co hydroxides.[19e] Reproduced with permission from the Royal Society of Chemistry (RSC).

$Co(OH)_{1.6}Cl_{0.4}\cdot 0.4\,H_2O$ (**7**) into **8** follows phase boundary control. Interestingly, the transformation of $Co(OH)_{1.5}(NO_3)_{0.5}\cdot 0.6\,H_2O$ (**6**) into **8** is accompanied by the occurrence of a crystalline intermediate which could be identified as α-$Co(OH)_2$ with Co^{2+} ion in a tetrahedral environment and a larger interlayer distance. The changes observed in the in-situ SAXS curves recorded during the conversion of **7** into **8** indicates that a large number of particles are formed at the very beginning of the transformation followed by a reduction of the particle number until a stationary state is reached. The alterations of the intensities in the SAXS and WAXS curves during the reaction are caused by Ostwald ripening, that is, larger and better crystalline particles grow at the expense of smaller ones. The results of the in-situ studies indicate that the phase conversions proceed by a dissolution–reconstruction mechanism.

3.1.5. *Formation of the Hybrid Compound $[Co(C_6H_{18}N_4)][Sb_2S_4]$*

Scattering experiments allow the characterization of particles over different length scales. But the species in solution and their local structure cannot be probed. The local and long-range structural information can be acquired combining X-ray absorption fine structure with X-ray scattering techniques. Applying this combination of analytical techniques, a sequence of reaction steps could be postulated for the hydrothermal crystallization of the layer compound $[Co(C_6H_{18}N_4)][Sb_2S_4]$.[7] In most syntheses the product reflections grow simultaneously after an induction period (Figure 8, top) while during some syntheses first only one reflection appeared and the remaining reflections occurred in the EDXRD spectra at a later stage (Figure 8, bottom).

The in-situ XAFS experiments performed on the Sb K-edge give strong indications that direct after the start of the reaction $[SbS_3/SbS_4]^{3-}$ ions are present in solution. These

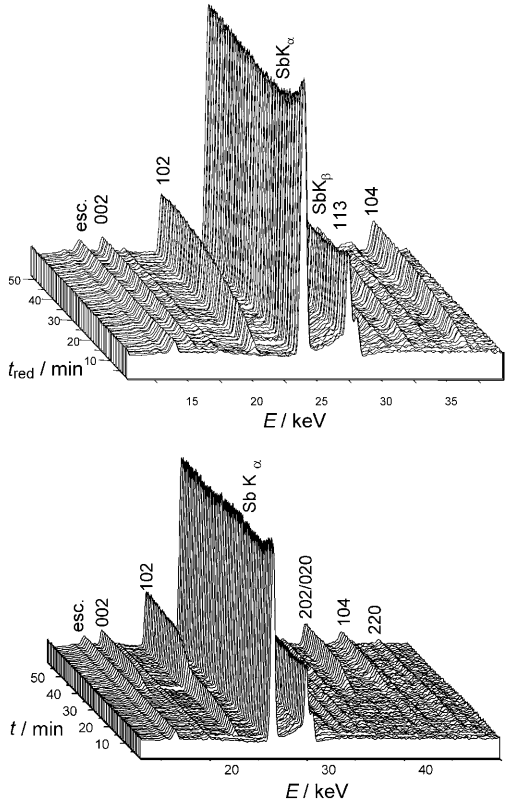

Figure 8. Time-resolved powder patterns of a reaction at 120 °C showing the different crystal-growth behavior of the hybrid compound. Top: typical example representing most of the synthesis; bottom: in about 1/3 of the experiments a different growth behavior is observed. The most intense reflections of the product $[Co(tren)][Sb_2S_4]$ and the $Sb_{K\alpha}$ fluorescence are marked and the escape peak is labeled with esc.[7] Reprinted with permission from Ref. [7]. Copyright 2011 American Chemical Society.

anions and the $[Co(C_6H_{18}N_4)]^{2+}$ ions in the solution condense to form single layers (Figure 9). The significant drop of the Sb K-edge signal is caused by the formation of an amorphous phase, which precipitated. Subsequently, after occurrence of the amorphous intermediate, either the product crystallizes

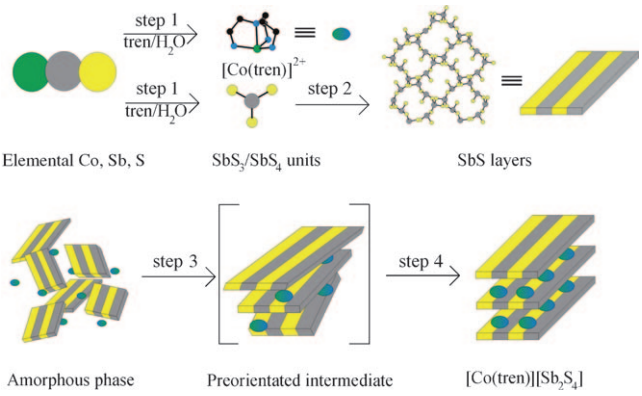

Figure 9. Formation mechanism of $[Co(C_6H_{18}N_4)][Sb_2S_4]$.[7] Co green, Sb gray, S yellow; tren = tris(2-aminoethyl)amine. Reprinted with permission from Ref. [7]. Copyright 2011 American Chemical Society.

directly (Figure 8, top and Figure 9) or a pre-oriented intermediate occurs which is transformed into the final long-range-ordered product by reorganization as the reaction progresses (Figure 9).

3.1.6. Zinc-Substituted Aluminophosphates

The whole length scale, starting from the atomic environment, over particle sizes, to the formation of crystallites can be probed simultaneously by applying combined in-situ SAXS, WAXS, and XAFS investigations. Such a combination of complementary methods was used to study the temperature dependent crystallization of a zinc-substituted aluminophosphate from a gel (Figure 10). The evaluation of the

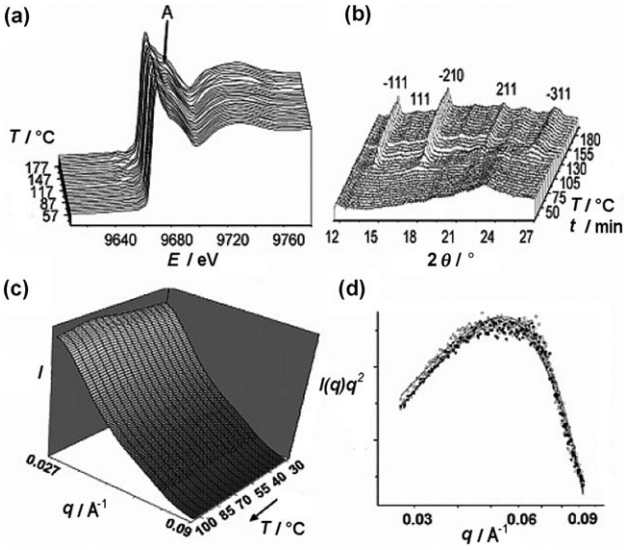

Figure 10. In-situ XANES (a), WAXS (b) and SAXS (c) curves recorded during the formation of the zinc-substituted aluminophosphates. The evaluation of the SAXS curve is displayed in (d). Reprinted with permission from Ref. [81]. Copyright 2011 American Chemical Society.

SAXS curves reveals that particle sizes increase only slightly from about 11.5 to 12.3 nm between 25 and 95 °C (start of crystallization, Figure 10c). The evaluation of the reflection widths in the WAXS patterns yields a value of about 12 nm for the crystallite sizes. Between 95 and 160 °C the crystallites grow further reaching a size of approximately 54 nm. The crystallization kinetics suggests a three-dimensional growth with decreasing nucleation rate. The XAFS spectra of the Zn K-edge clearly show the presence of Zn^{2+} ions in a tetrahedral environment during reaction. But just at the beginning of crystallization a change of the features of the Zn K-edge occurs which becomes more prominent during crystal growth (Figure 10a). The change is associated with the incorporation of the Zn^{2+} ions in the crystal structure. Before the appearance of the first reflections in the WAXS curve, the average particle size is about 12 nm, which is maintained after crystallization (Figure 10b). This observation can be explained with two scenarios: either critical nuclei were formed in the gel or a transition from an amorphous to a crystalline phase leads to the formation of the product. The Zn^{2+} ions seem to fulfill two different functions: they act as nucleation centers and they exert a structure-directing effect because the product does not crystallize with the expected AFI topology but with the cubic CHA topology.

3.2. Investigations of the Formation of Silicalites in Fluid Media

Before nucleation of a solid from a solution starts numerous complex reactions happen which proceed successively and/or parallel. The species involved in these reactions feature sizes between that of molecules and those of nanocrystallites and many in-situ techniques cannot probe such small objects. Such species in solution can be identified with in-situ mass spectrometry, and temporal as well as temperature-dependent alterations can be monitored. An example is the investigation of the mother liquids for the synthesis of silicalite-1 and silicalite-2.[53c] After ageing the liquids for 24 h at room temperature, the mass spectrum displays signals for a broad distribution of silicate species with masses up to *m*/*z* 2050. The most intense signal can be assigned to a silicate anion with composition $(Si_{32}O_{69}H_9)^-$ (a 32-mer). But no structural assignment is possible for this anion. Less intense signals arise from the prismatic hexamer $Si_6O_{15}H_5^-$ and the cubic octamer $Si_8O_{20}H_7^-$ (Figure 11a). In the mass spectrometer, reactions occur in the gas phase between the structure-

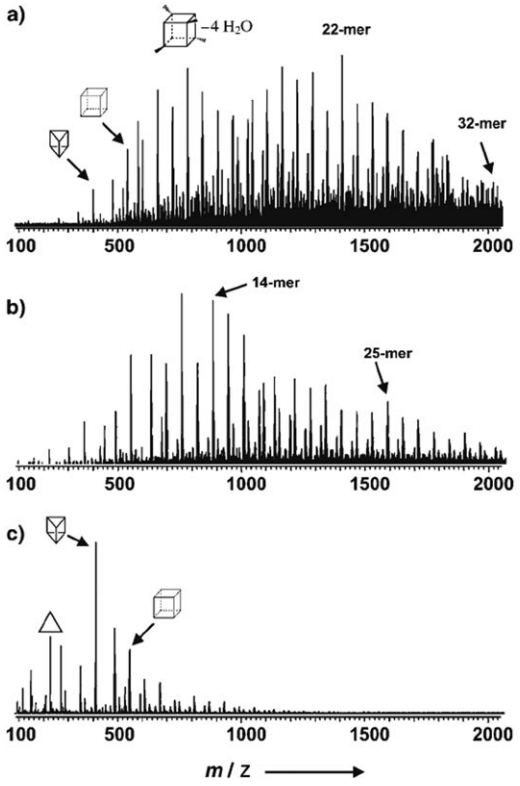

Figure 11. Mass spectra of the TEOS–TPAOH–H_2O mixture a) before heating, b) after 6 h, and c) after 61 h heating at 92 °C. The polyhedra show the shapes of the related silicate oligomers.[53c] TEOS = tetraethylorthosilicate, TPAOH = tetrapropylammoniumhydroxide.

directing molecules and the silicate species leading to satellites in the spectrum with defined mass differences. With increasing reaction time at 92 °C a significant shift toward lower masses is observed and after 61 h the hexamer is the most abundant species in solution (Figure 11 b,c). The simultaneous observation that the clear solution turned opaque is an indication for the formation of colloidal particles which could not be analyzed with the spectrometer used. The formation of zeolite crystals and of amorphous colloids leads to a reduction of the concentration of silicate species and structure-directing molecules in solution and accordingly to a depolymerization of oligomers. Furthermore, no dominating silicate species are detected in the mass spectra neither as transient nor as stationary species. Instead a broad distribution of diverse silicate building units is detected. All these results suggest that no distinct course of formation exists were a highly specific silicate unit is involved but rather the whole silicate-species pool acts as reservoir for crystal formation and growth. On the basis of these investigations it was not possible to decide whether monomers or different oligomers are the nucleation and crystallization centers. Because particles with sizes larger than about 1 nm exhibit huge masses beyond the mass limit of the spectrometer, the further growth could only be monitored with dynamic light scattering. It should be highlighted that on using a different structure-directing molecule, the same silicate species were identified but significantly differing kinetics of formation of these building units was observed.

3.3. Fast Precipitation Reaction in Solution

The precipitation of a solid in a solution is very often a rapid process and the early stages of particle formation such as shape, size, and growth cannot be monitored using slow methods such as light-scattering techniques. A specifically constructed flow-jet cell allowed the investigation of the precipitation of ZnS by in-situ SAXS (and also in-situ UV/Vis) on a μs scale (Figure 12).[82] A $ZnCl_2$ solution is injected into a H_2S atmosphere and the formation of ZnS is recorded along the jet stream, and after just 17 μs scattering by particles could be verified.

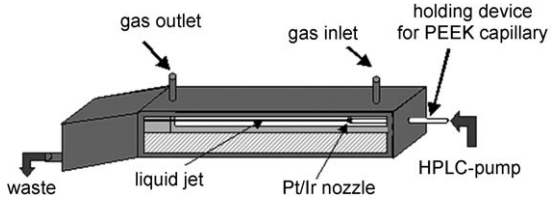

Figure 12. Schematic representation of the flow-jet cell. Reprinted with permission from Ref. [82]. Copyright 2011 American Chemical Society.

At the beginning, the particles are very small (Guinier approximation, $qR \ll 1$) and grow very fast from around 12 nm to about 25 nm within only 30 μs. By $t > 70$ μs the growth is so fast that now the Porod approximation ($qR \gg 1$) must be used for the interpretation of the data. The evaluation demonstrates that the density of the ZnS particles increases between 80 and 400 μs but the particle radius remains the same. This is a clear indication for further nucleation of ZnS but the growth of the particles is much slower. For $t > 400$ μs the particles become larger because of the increasing agglomeration rather than the growth of the crystallites.

3.4. Crystallization of Solids by Deposition at Low Temperatures

Theoretical calculation performed for LiBr revealed that it should be possible to kinetically stabilize polymorphs crystallizing in the wurtzite- or sphalerite-type structures as well as in the stable α-LiBr (NaCl structure; Figure 13).[66a]

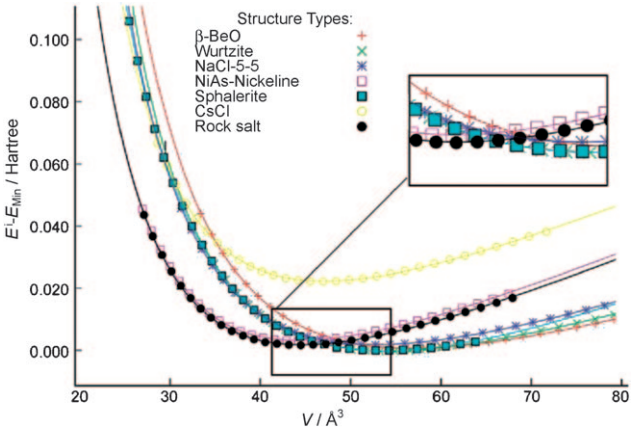

Figure 13. *E*/*V* curves of selected structure candidates with low energy on the LiBr energy landscape. The local optimization of each polymorph was carried out with ab-initio algorithms ($E_{Min=Wurzite} = -20.83888$ Hartree).[66a]

Indeed phase-pure β-LiBr with wurtzite-type structure could be prepared by depositing LiBr at low temperatures under a defined LiBr partial pressure. Using in-situ X-ray diffraction, the phase transition into the stable NaCl structure could be monitored (Figure 14). At −50 and −30 °C

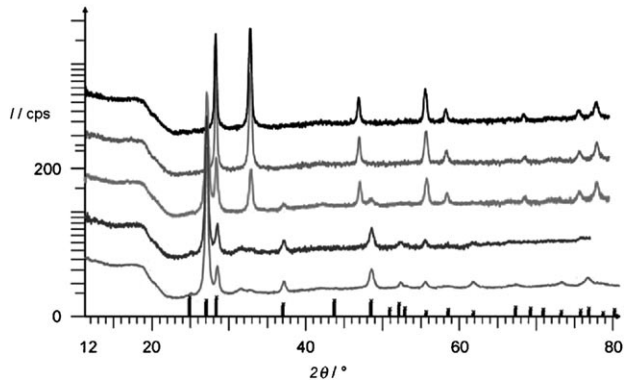

Figure 14. X-ray powder pattern of LiBr deposited at −50 °C). Patterns from top to bottom: −50 °C (wurtzite-type), −30 °C (wurtzite-type), −10 °C (wurtzite and NaCl structure), 10 °C and 25 °C (NaCl structure); thick vertical bars: β-LiBr.[66a]

(Figure 14) only reflections for β-LiBr are observed. On increasing the temperature to −10 °C (Figure 14) the reflections of both phases coexist and at 25 °C only α-LiBr can be identified. The phase transition is accompanied by a volume reduction of about 20 %, which is typical for the transformation of a metastable into the stable modification (Ostwald–Vollmer rule).

3.5. Crystallization of Solids from Gels

Yttrium-stabilized zirconium oxide exhibits a very high fracture toughness and a high strength, and is utilized for example, in machinery construction and in forming processes. Owing to its excellent biocompatibility, stabilized ZrO_2 is also applied in the prosthetic dentistry. Pure ZrO_2 is polymorphic and doping with about 3 mol % Y_2O_3 stabilizes the metastable tetragonal modification at room temperature and at higher doping levels the high-temperature cubic form can be stabilized at room temperature. The crystallization of yttrium-stabilized ZrO_2 from a gel was studied with ASAXS and the evaluation of the data yields a comprehensive picture of the temperature-dependent formation.[83] A xerogel pellet was used as the starting material and heated to 1000 °C with a heating rate of 10 °C min^{-1}. The ASAXS curves were collected at six different energies with a time resolution of about 20 s. The results are schematically summarized in Figure 15. At the beginning Zr and Y primary particles with

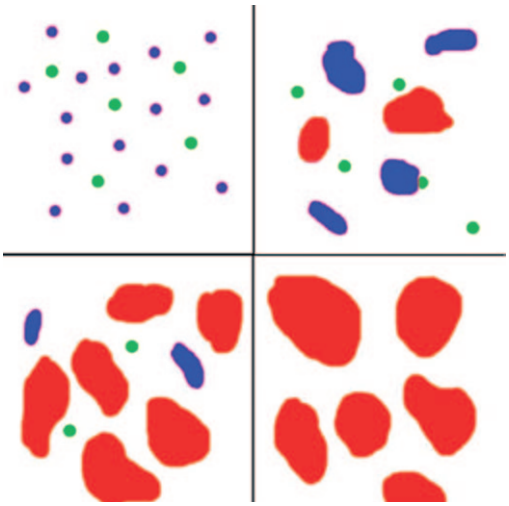

Figure 15. Reaction scheme for the formation of yttrium-stabilized ZrO_2.[83] Y primary particles (green), Zr primary particles (blue), Y-stabilized ZrO_2 (red). See text for details. Reprinted with permission from Ref. [83]. Copyright 2011 American Chemical Society.

sizes of 1–2 nm are homogeneously distributed in the xerogel (Figure 15, top left). At about 380 °C nucleation of zirconium-containing particles with the tetragonal ZrO_2 modification occurs which then grow (Figure 15, top right) integrating yttrium-containing particles in the ZrO_2 matrix (Figure 15, bottom left). During Y uptake a phase transition into the cubic modification occurs, that is, in a distinct temperature range inhomogeneities are present which disappear when Y is completely incorporated in the ZrO_2 matrix (Figure 15, bottom right). The nucleation of ZrO_2 is accompanied by a pronounced increase of the particle size (Figure 15, top left and right).

3.6. Reactions between Solids and Gases

Anionic conductors are employed in different areas such as fuel cells or in lambda probes. In these materials the O^{2-} ions are mobile at elevated temperatures. For special applications, materials with a high mobility of N^{3-} ions are of great interest, these may be occur in oxynitrides. Gallium oxide Ga_2O_3 can be transformed to GaN in an ammonia atmosphere at elevated temperatures. An interesting question is whether intermediate gallium oxynitrides are formed during the reaction, which could be mixed anionic conductors. Using time-resolved in-situ EXAFS during the ammonolysis of Ga_2O_3 (Figure 16; QEXAFS mode, $T = 660$–840 °C) it

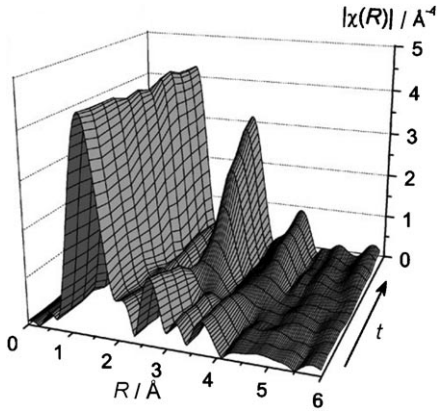

Figure 16. Change of the radial EXAFS distribution recorded during ammonolysis of Ga_2O_3 at 780 °C.[84] Reproduced with permission from the Royal Society of Chemistry (RSC).

could be demonstrated that Ga_2O_3 and GaN are always simultaneously present until full conversion to GaN is reached, that is, no additional phases appear.[84] In Figure 16 it can clearly be seen that during the reaction only small changes occur in the first coordination shell around Ga. In contrast, pronounced alterations are observed for the second shell caused by the different environments of Ga in GaN and Ga_2O_3. In GaN the Ga atom has a clearly defined second coordination shell consisting of 12 Ga neighbors at 3.18 Å, while the second shell around Ga in Ga_2O_3 is relatively "diffuse" containing 20 Ga neighbors at a distance between 3.04 and 3.44 Å. The rate-limiting step of the reaction is the formation of GaN at the interface between the GaN nuclei and the Ga_2O_3 matrix. In ex-situ recorded TEM micrographs GaN nuclei could be identified. The oxidation of GaN to Ga_2O_3 proceeds by shrinking of the GaN particle core (Figure 17) and the formation of Ga_2O_3 at the interface to GaN is the rate-determining step of the reaction.

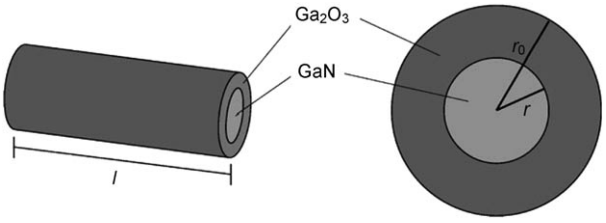

Figure 17. Schematic illustration of the reaction path from GaN to Ga_2O_3. With increasing reaction time the size of the GaN core is reduced.[84] Reproduced with permission from the Royal Society of Chemistry (RSC).

3.7. Solid–Solid Reactions

Self-propagating high-temperature syntheses (SHS) are promising methods for the preparation of alloys and high-temperature ceramics.[85] The in-situ investigation of SHS reactions is challenging owing to the very fast reaction rate. Recently the reaction of Al with Ni was investigated by in-situ X-ray scattering with a time resolution of 100 ms (Figure 18).[86]

First a powder pattern was recorded at room temperature then the reaction was initiated. During the reaction, 120 patterns were collected within 16.2 seconds and another pattern was recorded at the end of the reaction. After start of the reaction, a temperature of about 1550 °C is reached within 200 ms. The reaction can be divided into different stages:

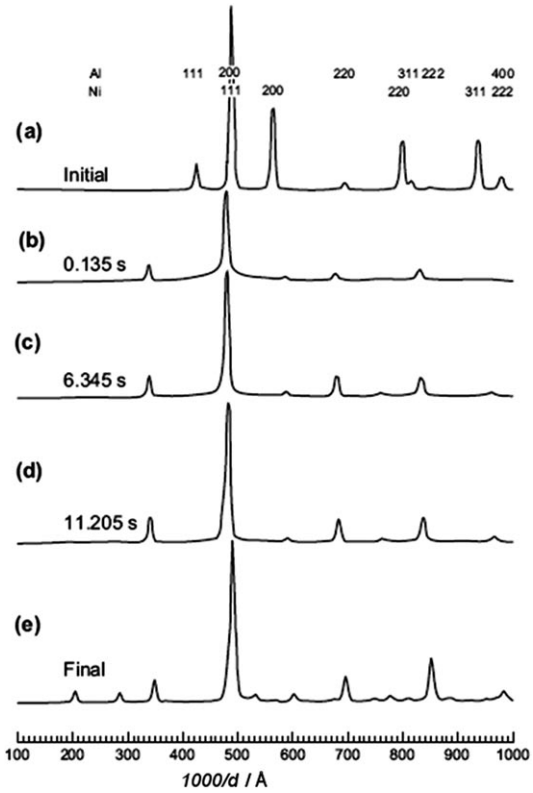

Figure 18. Powder patterns recorded during a typical SHS experiment of a Al–Ni sample, see text for details.[86] Reprinted from Ref. [86], Copyright 2011, with permission from Elsevier.

between $t = 0$ and 0.135 s reflections of Al and Ni disappears, the background increases, and new reflections of AlNi can be identified. Between 0.135 and 6.345 s the reflection positions of AlNi shift and the intensity of the reflections increase; in addition some weak extra reflections appear, which can be indexed on the basis of Al_3Ni. The (110) reflection of AlNi becomes broader and asymmetric, the background in the pattern decreases. Between $t = 6.345$ and 11.205 s all the reflections shift towards lower d-values accompanied by a slight increase of the intensities and new reflections of Al_3Ni_2 start to grow. At the end of the reaction a mixture is found composed of AlNi and Al_3Ni_2 with small amounts of Al_3Ni and Al_3Ni_5. The results suggest the following scenario for the reaction: melting of Al initiated the reaction and the temperature of 1550 °C is near the melting point of AlNi and higher than the melting points of all other Al–Ni phases. During cooling the different phases crystallize and because heating and cooling processes are too fast no equilibrium is reached.

4. Summary and Outlook

During the last few years a dynamic development has taken place in instrumentation, both of laboratory equipment as well as of major research institutions. Hence, powerful in-situ methods are available to investigate the formation of solids, in an element-specific way, under real reaction conditions, on different time and lengths scales. But many experiments can only be performed if the required sample environment is available. As mentioned above such apparatus have to be designed and built which requires the logistics and the appropriate equipment. But the examples presented herein demonstrate that in-situ investigations contribute significantly to a better understanding of the formation of crystalline solids. Even the study of a reaction with only one method may lead to a comprehensive picture about the course of the crystallization of a solid. For a clearer understanding about the formation of crystalline solids complementary methods that are sensitive towards different stages of crystal formation should be used, that is, the information content increases with increasingly complementary in-situ experiments. But it must be noted that at the same time, the time scale and the experimental effort significantly increase, which must be considered during the planning phase of an experiment. Moreover, the level of expenditure compared to the value of the results should be carefully considered. When performing experiments with synchrotron radiation it is essential to remember that the intense radiation is focused on a diameter of a few μm which may influence chemical reactions in an unwanted way.[87]

Despite the increase of in-situ studies we are far away from formulating a thorough view of the formation of crystalline solids or "designing" such crystalline solids. Nevertheless, this is not surprising considering the large number of crystalline materials, their variable chemical compositions, and the multitude of synthetic methods. Every result of an in-situ investigation may add a small piece in an immense jigsaw puzzle. Compared to the enormous number of publications reporting the synthesis and characterization of a new

crystalline solids, the number of reports about in-situ studies of the formation of crystalline solids is still very small. Hence, it is desirable and our opinion that many more such in-situ experiments should be performed. The necessity to perform in-situ studies using different combinations of analytical techniques[88] was recognized a long time ago in the area of catalysis. The results of these experiments significantly enhanced the understanding of catalytic reactions.

The necessity to pool the skills of scientists of different scientific areas in a nationwide program was recognized in Great Britain a couple of years ago (Basic Technology Programme "Control and Prediction of the Organic Solid State"; cposs). Recently, a new project was launched in Germany where the fundamental steps of the formation of crystalline solids (model compounds) should be investigated experimentally and theoretically. In the priority program 1415 of the German Science Foundation (DFG), with the title "Crystalline Non-Equilibrium Phases—Synthesis, Characterization, and In-Situ Investigation of Formation Mechanisms", the necessary basic information for more directed syntheses of metastable crystalline solids should be developed. In a subproject a new in-situ cell is to be developed for the investigation and control of crystallization. This cell is to be used by all the participants of the program. At first the cell is used for investigations in fluid media and is equipped with measuring probes recording and regulating simultaneously parameters including temperature, pressure, pH value, conductivity, redox potential, and concentration.

New developments in the area of size- and time-resolved methods like nonlinear optical spectroscopy (NLO, second harmonic generation, hyper-Raleigh-scattering) may be additional important steps for the investigation of formation of crystalline solids. Several publications about the investigation of colloidal interfaces,[89] the formation of amphiphilic polyester micelles,[90] or the time-resolved investigation of the crystallization of ZnO in the sub 10 nm region[91] demonstrate the large potential of these optical methods. The advancement of the analysis of optical absorption spectra allows the determination of size distribution, solubility, and surface energy of particles in the nanoscopic regime, that is, at the beginning of the formation of a crystalline solid.[92]

The information gap between X-ray scattering (long-range, crystalline state) and XAFS (local environment) may be closed using pair distribution function (PDF) analyses. This method has been applied to the analysis of solids for several years,[93] but to date it is not used for in-situ experiments. But it can be expected that more in-situ scattering experiments will be performed in the near future due to the development of very sensitive and fast detectors like the Pilatus detectors.

We thank Priv.-Doz. Dr. C. Näther for fruitful discussions and suggestions. Financial support by the State of Schleswig-Holstein and the Deutsche Forschungsgemeinschaft (DFG) are gratefully acknowledged.

Received: February 26, 2010
Published online: February 15, 2011

[1] D. Erdemir, A. Y. Lee, A. S. Myerson, *Acc. Chem. Res.* **2009**, *42*, 621 – 629.

[2] a) D. M. Herlach, I. Klassen, P. Wette, D. Holland-Moritz, *J. Phys. Condens. Matter* **2010**, *22*, 153101; b) D. J. W. Aastuen, N. A. Clark, L. K. Cotter, *Phys. Rev. Lett.* **1986**, *57*, 1733 – 1736; c) C. D. Dushkin, H. Yoshimura, K. Nagayama, *Chem. Phys. Lett.* **1993**, *204*, 455 – 460; d) T. H. Zhang, X. Y. Liu, *Angew. Chem.* **2009**, *121*, 1334 – 1338; *Angew. Chem. Int. Ed.* **2009**, *48*, 1308 – 1312; e) U. Gasser, *J. Phys. Condens. Matter* **2009**, *21*, 203101; f) A. Yethiraj, A. van Blaaderen, *Nature* **2003**, *421*, 513 – 517; g) A. van Blaaderen, R. Ruel, P. Wiltzius, *Nature* **1997**, *385*, 321 – 324; h) W. B. Russel, *Nature* **2003**, *421*, 490 – 491; i) K. P. Velikov, C. G. Christova, R. P. A. Dullens, A. van Blaaderen, *Science* **2002**, *296*, 106 – 109; j) C. P. Royall, M. E. Leunissen, A. van Blaaderen, *J. Phys. Condens. Matter* **2003**, *15*, S3581-S3596; k) T. H. Zhang, X. Y. Liu, *J. Phys. Chem. B* **2007**, *111*, 14001 – 14005; l) M. E. Leunissen, C. G. Christova, A.-P. Hynninen, C. P. Royall, A. I. Campbell, A. Imhof, M. Dijkstra, R. van Roij, A. van Blaaderen, *Nature* **2005**, *437*, 235 – 240.

[3] a) V. W. A. de Villeneuve, D. Verboekend, R. P. A. Dullens, D. G. A. L. Aarts, W. K. Kegel, H. N. W. Lekkerkerker, *J. Phys. Condens. Matter* **2005**, *17*, S3371 – S3378; b) T. Gong, J. Shen, Z. Hu, M. Marquez, Z. Cheng, *Langmuir* **2007**, *23*, 2919 – 2923; c) N. Geerts, S. Jahn, E. Eiser, *J. Phys. Condens. Matter* **2010**, *22*, 104111 – 104116; d) P. Schall, I. Cohen, D. A. Weitz, F. Spaepen, *Nature* **2006**, *440*, 319 – 323; e) S. Auer, D. Frenkel, *Annu. Rev. Phys. Chem.* **2004**, *55*, 333 – 361; f) A.-P. Hynninen, M. E. Leunissen, A. van Blaaderen, M. Dijkstra, *Phys. Rev. Lett.* **2006**, *96*, 018303; g) R. Prieler, J. Hubert, D. Li, B. Verleye, R. Haberkern, H. Emmerich, *J. Phys. Condens. Matter* **2009**, *21*, 464110; h) S. Auer, D. Frenkel, *Adv. Polym. Sci.* **2005**, *173*, 149 – 207; i) M. Marechal, M. Dijkstra, *Phys. Rev. E* **2007**, *75*, 061404; j) H. J. Schöpe, G. Bryant, M. van Megen, *Phys. Rev. Lett.* **2006**, *96*, 175701.

[4] a) M. Jansen, *Angew. Chem.* **2002**, *114*, 3896 – 3917; *Angew. Chem. Int. Ed.* **2002**, *41*, 3746 – 3766; b) J. C. Schön, M. Jansen, *Angew. Chem.* **1996**, *108*, 1358 – 1377; *Angew. Chem. Int. Ed. Engl.* **1996**, *35*, 1286 – 1304; c) J. C. Schön, M. Jansen, *Z. Kristallogr.* **2001**, *216*, 307 – 325.

[5] a) J. Bernstein, J. O. Henck, *Mater. Res. Bull.* **1998**, *33 Suppl. S*, 119 – 128; b) J. D. Dunitz, J. Bernstein, *Acc. Chem. Res.* **1995**, *28*, 193 – 200; c) J. O. Henck, J. Bernstein, A. Ellern, R. Boese, *J. Am. Chem. Soc.* **2001**, *123*, 1834 – 1841.

[6] a) L. Engelke, M. Schaefer, M. Schur, W. Bensch, *Chem. Mater.* **2001**, *13*, 1383 – 1390; b) L. Engelke, M. Schaefer, F. Porsch, W. Bensch, *Eur. J. Inorg. Chem.* **2003**, 506 – 513; c) N. Pienack, C. Näther, W. Bensch, *Eur. J. Inorg. Chem.* **2009**, 937 – 946.

[7] R. Kiebach, N. Pienack, M. E. Ordolff, F. Studt, W. Bensch, *Chem. Mater.* **2006**, *18*, 1196 – 1205.

[8] a) A. Michailovski, J. D. Grunwaldt, A. Baiker, R. Kiebach, W. Bensch, G. R. Patzke, *Angew. Chem.* **2005**, *117*, 5787 – 5792; *Angew. Chem. Int. Ed.* **2005**, *44*, 5643 – 5647; b) A. Michailovski, R. Kiebach, W. Bensch, J. D. Grunwaldt, A. Baiker, S. Komarneni, G. R. Patzke, *Chem. Mater.* **2007**, *19*, 185 – 197; c) R. Kiebach, N. Pienack, W. Bensch, J. D. Grunwaldt, A. Michailovski, A. Baiker, T. Fox, Y. Zhou, G. R. Patzke, *Chem. Mater.* **2008**, *20*, 3022 – 3033; d) F. Millange, M. I. Medina, N. Guillou, G. Férey, K. M. Golden, R. I. Walton, *Angew. Chem.* **2010**, *122*, 775 – 778; *Angew. Chem. Int. Ed.* **2010**, *49*, 763 – 766.

[9] a) J. M. Thomas, *Angew. Chem.* **1999**, *111*, 3800 – 3843; *Angew. Chem. Int. Ed.* **1999**, *38*, 3588 – 3628; b) T. Shido, R. Prins, *Curr. Opin. Solid State Mater. Sci.* **1998**, *3*, 330 – 335; c) M. Erko, D. Wallacher, A. Brandt, O. Paris, *J. Appl. Crystallogr.* **2010**, *43*, 1 – 7; d) A. Y. Khodakov, V. L. Zholobenko, M. Imperor-Clerc, D. Durand, *J. Phys. Chem. B* **2005**, *109*, 22780 – 22790; e) G. D.

Wignall, Y. B. Melnichenko, *Rep. Prog. Phys.* **2005**, *68*, 1761 – 1810.

[10] a) P. Barnes, S. M. Clark, D. Häusermann, E. Henderson, C. H. Fentiman, M. N. Muhamad, S. Rashid, *Phase Transitions* **1992**, *39*, 117 – 128; b) J. Munn, P. Barnes, D. Häusermann, S. A. Axon, J. Klinowski, *Phase Transitions* **1992**, *39*, 129 – 134; c) H. He, P. Barnes, J. Munn, X. Turrillas, J. Klinowski, *Chem. Phys. Lett.* **1992**, *196*, 267 – 273; d) J. W. Couves, J. M. Thomas, D. Waller, R. H. Jones, A. J. Dent, G. E. Derbyshire, G. N. Greaves, *Nature* **1991**, *354*, 465 – 468; e) J. M. Thomas, G. N. Greaves, *Science* **1994**, *265*, 1675 – 1676.

[11] a) R. I. Walton, T. Loiseau, D. O'Hare, G. Ferey, *Chem. Mater.* **1999**, *11*, 3201 – 3209; b) R. I. Walton, A. J. Norquist, S. Neeraj, S. Natarajan, C. N. R. Rao, D. O'Hare, *Chem. Commun.* **2001**, 1990 – 1991; c) P. Norby, A. N. Christensen, J. C. Hanson, *Inorg. Chem.* **1999**, *38*, 1216 – 1221; d) J. Wienold, O. Timpe, T. Ressler, *Chem. Eur. J.* **2003**, *9*, 6007 – 6017.

[12] a) R. I. Walton, D. O'Hare, *Chem. Commun.* **2000**, 2283 – 2291; b) T. Ressler, *Anal. Bioanal. Chem.* **2003**, *376*, 584 – 593; c) A. N. Christensen, P. Norby, J. C. Hanson, *J. Solid State Chem.* **1995**, *114*, 556 – 559.

[13] a) G. Sandí, R. E. Winans, S. Seifert, K. A. Carrado, *Chem. Mater.* **2002**, *14*, 739 – 742; b) J. Morell, C. V. Teixeira, M. Cornelius, V. Rebbin, M. Tiemann, H. Amenitsch, M. Fröba, M. Lindén, *Chem. Mater.* **2004**, *16*, 5564 – 5566; c) K. Flodström, C. V. Teixeira, H. Amenitsch, V. Alfredsson, M. Linden, *Langmuir* **2004**, *20*, 4885 – 4891; d) C. H. Cheng, D. F. Shantz, *J. Phys. Chem. B* **2005**, *109*, 13912 – 13920.

[14] a) A. T. Davies, G. Sankar, C. R. A. Catlow, S. M. Clark, *J. Phys. Chem. B* **1997**, *101*, 10115 – 10120; b) A. Gualtieri, P. Norby, G. Artioli, J. Hanson, *Phys. Chem. Miner.* **1997**, *24*, 191 – 199; c) R. I. Walton, F. Millange, D. O'Hare, A. T. Davies, G. Sankar, C. R. A. Catlow, *J. Phys. Chem. B* **2001**, *105*, 83 – 90; d) R. I. Walton, D. O'Hare, *J. Phys. Chem. B* **2001**, *105*, 91 – 96.

[15] L. M. Colyer, G. N. Greaves, A. J. Dent, K. K. Fox, S. W. Carr, R. H. Jones, *Nucl. Instrum. Methods Phys. Res. Sect. B* **1995**, *97*, 107 – 110.

[16] P. Norby, *J. Am. Chem. Soc.* **1997**, *119*, 5215 – 5221.

[17] a) F. Rey, G. Sankar, J. M. Thomas, P. A. Barrett, D. W. Lewis, C. R. A. Catlow, *Chem. Mater.* **1995**, *7*, 1435 – 1436; b) R. J. Francis, S. J. Price, S. O'Brien, A. M. Fogg, D. O'Hare, T. Loiseau, G. Férey, *Chem. Commun.* **1997**, 521 – 522; c) P. Norby, J. C. Hanson, *Catal. Today* **1998**, *39*, 301 – 309; d) A. N. Christensen, T. R. Jensen, P. Norby, J. C. Hanson, *Chem. Mater.* **1998**, *10*, 1688 – 1693; e) R. J. Francis, S. O'Brien, A. M. Fogg, P. S. Halasyamani, D. O'Hare, T. Loiseau, G. Férey, *J. Am. Chem. Soc.* **1999**, *121*, 1002 – 1015; f) R. I. Walton, A. Norquist, R. I. Smith, D. O'Hare, *Faraday Discuss.* **2003**, *122*, 331 – 341; g) F. Millange, R. I. Walton, N. Guillou, T. Loiseau, D. O'Hare, G. Férey, *Chem. Commun.* **2002**, 826 – 827; h) G. Muncaster, A. T. Davies, G. Sankar, C. R. A. Catlow, J. M. Thomas, S. L. Colston, P. Barnes, R. I. Walton, D. O'Hare, *Phys. Chem. Chem. Phys.* **2000**, *2*, 3523 – 3527.

[18] a) R. J. Francis, S. J. Price, J. S. O. Evans, S. O'Brien, D. O'Hare, S. M. Clark, *Chem. Mater.* **1996**, *8*, 2102 – 2108; b) H. Ahari, A. Lough, S. Petrov, G. A. Ozin, R. L. Bedard, *J. Mater. Chem.* **1999**, *9*, 1263 – 1274.

[19] a) A. K. Cheetham, C. F. Mellot, *Chem. Mater.* **1997**, *9*, 2269 – 2279; b) W. H. Dokter, T. P. M. Beelen, H. F. van Garderen, R. A. van Santen, W. Bras, G. E. Derbyshire, G. R. Mant, *J. Appl. Crystallogr.* **1994**, *27*, 901 – 906; c) K. Shinoda, E. Matsubara, M. Saito, Y. Waseda, T. Hirato, Y. Awakura, *Z. Naturforsch. B* **1997**, *52*, 855 – 862; d) S. Connolly, S. Fullam, B. Korgel, D. Fitzmaurice, *J. Am. Chem. Soc.* **1998**, *120*, 2969 – 2970; e) Y. Du, K. M. Ok, D. O'Hare, *J. Mater. Chem.* **2008**, *18*, 4450 – 4459; f) C. L. Cahill, L. G. Benning, H. L. Barnes, J. B. Parise, *Chem. Geol.* **2000**, *167*, 53 – 63; g) R. Kiebach, M. Schaefer, F. Porsch, W. Bensch, *Z. Anorg. Allg. Chem.* **2005**, *631*, 369 – 374; h) Y. Zhou, N. Pienack, W. Bensch, G. R. Patzke, *Small* **2009**, *5*, 1978 – 1983; i) A. N. Christensen, T. R. Jensen, N. V. Y. Scarlett, I. C. Madsen, J. C. Hanson, A. Altomare, *Dalton Trans.* **2003**, 3278 – 3282; j) D. R. Modeshia, R. J. Darton, S. E. Ashbrook, R. I. Walton, *Chem. Commun.* **2009**, 68 – 70; k) R. D. Fisher, R. I. Walton, *Dalton Trans.* **2009**, 8079 – 8086; l) A. M. Beale, G. Sankar, *Chem. Mater.* **2006**, *18*, 263 – 272; m) H. P. Vu, S. Shaw, L. Brinza, L. G. Benning, *Cryst. Growth Des.* **2010**, *10*, 1544 – 1551.

[20] a) W. Paulus, H. Katzke, R. Schöllhorn, *J. Solid State Chem.* **1992**, *96*, 162 – 168; b) S. M. Clark, P. Irvin, J. Flaherty, T. Rathbone, H. V. Wong, J. S. O. Evans, D. O'Hare, *Rev. Sci. Instrum.* **1994**, *65*, 2210 – 2213; c) J. S. O. Evans, R. J. Francis, D. O'Hare, S. J. Price, S. M. Clark, J. Flaherty, J. Gordon, A. Nield, C. C. Tang, *Rev. Sci. Instrum.* **1995**, *66*, 2442 – 2445; d) S. M. Clark, J. S. O. Evans, D. O'Hare, C. J. Nuttall, H. V. Wong, *J. Chem. Soc. Chem. Commun.* **1994**, 809 – 810; e) J. S. O. Evans, S. J. Price, H.-V. Wong, D. O'Hare, *J. Am. Chem. Soc.* **1998**, *120*, 10837 – 10846; f) J. S. O. Evans, D. O'Hare, *Adv. Mater.* **1994**, *6*, 646 – 648; g) A. M. Fogg, D. O'Hare, *Chem. Mater.* **1999**, *11*, 1771 – 1775; h) A. M. Fogg, S. J. Price, R. J. Francis, S. O'Brien, D. O'Hare, *J. Mater. Chem.* **2000**, *10*, 2355 – 2357; i) J. S. C. Loh, A. M. Fogg, H. R. Watling, G. M. Parkinson, D. O'Hare, *Phys. Chem. Chem. Phys.* **2000**, *2*, 3597 – 3604; j) F. Millange, R. I. Walton, D. O'Hare, *J. Mater. Chem.* **2000**, *10*, 1713 – 1720; k) G. R. Williams, A. J. Norquist, D. O'Hare, *Chem. Commun.* **2003**, 1816 – 1817; l) M. Behrens, R. Kiebach, J. Ophey, O. Riemenschneider, W. Bensch, *Chem. Eur. J.* **2006**, *12*, 6348 – 6355; m) J. Wontcheu, M. Behrens, W. Bensch, S. Indris, M. Wilkening, P. Heitjans, *Solid State Ionics* **2007**, *178*, 759 – 768; n) A. J. Celestian, J. B. Parise, C. Goodell, A. Tripathi, J. Hanson, *Chem. Mater.* **2004**, *16*, 2244 – 2254.

[21] a) T. Atou, J. V. Badding, *J. Solid State Chem.* **1995**, *118*, 299 – 302; b) M. Epple, G. Sankar, J. M. Thomas, *Chem. Mater.* **1997**, *9*, 3127 – 3131; c) T. Ressler, R. E. Jentoft, J. Wienold, M. M. Günter, O. Timpe, *J. Phys. Chem. B* **2000**, *104*, 6360 – 6370.

[22] A. E. Terry, G. B. M. Vaughan, A. Kvick, R. I. Walton, A. J. Norquist, D. O'Hare, *Synchrotron Radiat. News* **2002**, *15*, 4 – 13.

[23] a) D. E. Sayers, E. A. Stern, F. Lytle, *Phys. Rev. Lett.* **1971**, *27*, 1204 – 1207; b) D. E. Sayers, F. W. Lytle, M. Weissbluth, P. Pianetta, *J. Chem. Phys.* **1975**, *62*, 2514 – 2515; c) P. A. Lee, J. B. Pendry, *Phys. Rev. B* **1975**, *11*, 2795 – 2811; d) F. W. Lytle, D. E. Sayers, E. A. Stern, *Phys. Rev. B* **1975**, *11*, 4825 – 4835; e) E. A. Stern, D. E. Sayers, F. W. Lytle, *Phys. Rev. B* **1975**, *11*, 4836 – 4846; f) B. K. Teo in *EXAFS: Basic Principles and Data Analysis*, Springer, Berlin, **1986**.

[24] S. Pascarelli, O. Mathon, M. Munoz, T. Mairs, J. Susini, *J. Synchrotron Radiat.* **2006**, *13*, 351 – 358.

[25] a) M. Bauer, H. Bertagnolli, *ChemPhysChem* **2009**, *10*, 2197 – 2200; b) C. Bressler, C. Milne, V. T. Pham, A. ElNahhas, R. M. van der Veen, W. Gawelda, S. Johnson, P. Beaud, D. Grolimund, M. Kaiser, C. N. Borca, G. Ingold, R. Abela, M. Chergui, *Science* **2009**, *323*, 489 – 492; c) M. Bargheer, N. Zhavoronkov, M. Woerner, T. Elsaesser, *ChemPhysChem* **2006**, *7*, 783 – 792; d) K. J. Gaffney, H. N. Chapman, *Science* **2007**, *316*, 1444 – 1448.

[26] a) O. Glatter, K. C. Holmes, R. Kirste, G. Kostorz, O. Kratky, R. Laggner, H. Leopold, K. Müller, R. C. Oberthür, I. Pilz, G. Porod, H. Stuhrmann, C. G. Vonk, P. Zipper in *Small Angle X-Ray Scattering* (Eds.: O. Glatter, O. Kratky), Academic Press, London, **1982**; b) A. Guinier, G. Fournet in *Small Angle Scattering of X-Rays*, VCH, New York, **1955**.

[27] http://lamp.tu-graz.ac.at/~nanoanal/de/methoden_popup.php?id=1037. Prof. Dr. Peter Laggner, IBN, Institut für Biophysik und Nanosystemforschung, Österreichische Akademie der Wissenschaften (http://www.oeaw.ac.at).

[28] U. Vainio, DESY Summer School Lectures **2009**.

[29] D. I. Svergun, M. H. J. Koch, *Rep. Prog. Phys.* **2003**, *66*, 1735 – 1782.

[30] a) G. Goerigk, H. G. Haubold, O. Lyon, J. P. Simon, *J. Appl. Crystallogr.* **2003**, *36*, 425 – 429; b) H. G. Haubold, R. Gebhardt, G. Buth, G. Goerigk in *Resonant Anomalous X-Ray Scattering* (Eds.: G. Materlik, C. J. Sparks, K. Fischer), Elsevier, Dordrecht, **1994**, pp. 295 – 304.

[31] a) U. S. Jeng, C. H. Su, C. J. Su, K. F. Liao, W. T. Chuang, Y. H. Lai, J. W. Chang, Y. J. Chen, Y. S. Huang, M. T. Lee, K. L. Yu, J. M. Lin, D. G. Liu, C. F. Chang, C. Y. Liu, C. H. Chang, K. S. Liang, *J. Appl. Crystallogr.* **2010**, *43*, 110 – 121; b) Y. H. Lai, Y. S. Sun, U. S. Jeng, J. M. Lin, T. L. Lin, H. S. Sheu, W. T. Chuang, Y. S. Huang, C. H. Hsu, M. T. Lee, H. Y. Lee, K. S. Liang, A. Gabriel, M. H. J. Koch, *J. Appl. Crystallogr.* **2006**, *39*, 871 – 877; c) S. Nikitenko, A. M. Beale, A. M. J. van der Eerden, S. D. M. Jacques, O. Leynaud, M. G. O'Brien, D. Detollenaere, R. Kaptein, B. M. Weckhuysen, W. Bras, *J. Synchrotron Radiat.* **2008**, *15*, 632 – 640.

[32] D. Le Messurier, R. Winter, C. M. Martin, *J. Appl. Crystallogr.* **2006**, *39*, 589 – 594.

[33] K. A. Carrado, L. Xu, D. M. Gregory, K. Song, S. Seifert, R. E. Botto, *Chem. Mater.* **2000**, *12*, 3052 – 3059.

[34] a) C. H. Sheng, D. F. Shantz, *J. Phys. Chem. B* **2005**, *109*, 13912 – 13920; b) P. P. E. A. de Moor, T. P. M. Beelen, B. U. Komanschek, O. Diat, R. A. van Santen, *J. Phys. Chem. B* **1997**, *101*, 11077 – 11086; c) P. P. E. A. de Moor, T. P. M. Beelen, R. A. van Santen, *Microporous Mater.* **1997**, *9*, 117 – 130; d) P. P. E. A. de Moor, T. P. M. Beelen, R. A. van Santen, *J. Phys. Chem. B* **1999**, *103*, 1639 – 1650; e) J. N. Watson, L. E. Iton, R. I. Keir, J. C. Thomas, T. L. Dowling, J. W. White, *J. Phys. Chem. B* **1997**, *101*, 10094 – 10104; f) S. Yang, A. Navrotsky, D. Wesolowski, J. A. Pople, *Chem. Mater.* **2004**, *16*, 210 – 219.

[35] J. Pannetier, in *Chemical Crystallography with Pulsed Neutrons and Synchrotron X-rays*, *Vol. 22*1 (Eds.: N. A. Carrondo, G. A. Jeffrey), NATO Advanced Study Institute, Reidel, Dordrecht, **1988**, p. 313.

[36] E. Polak, J. Munn, P. Barnes, S. E. Tarling, C. Ritter, *J. Appl. Crystallogr.* **1990**, *23*, 258 – 262.

[37] a) X. Turrillas, P. Barnes, D. Gascoigne, J. Z. Turner, S. L. Jones, C. J. Norman, C. F. Pygall, A. J. Dent, *Radiat. Phys. Chem.* **1995**, *45*, 491 – 508; b) X. Turrillas, P. Barnes, S. E. Tarling, S. L. Jones, C. J. Norman, C. Ritter, *J. Mater. Sci. Lett.* **1993**, *12*, 223 – 226.

[38] H. Kohlmann, N. Kurtzemann, R. Weihrich, T. Hansen, *Z. Anorg. Allg. Chem.* **2009**, *635*, 2399 – 2405.

[39] a) L. E. Iton, F. Trouw, T. O. Brun, J. E. Epperson, J. W. White, S. J. Henderson, *Langmuir* **1992**, *8*, 1045 – 1048; b) J. Dougherty, L. E. Iton, J. W. White, *Zeolites* **1995**, *15*, 640 – 649; c) J. N. Watson, L. E. Iton, J. W. White, *Chem. Commun.* **1996**, 2767 – 2768; d) R. I. Walton, F. Millange, R. I. Smith, T. C. Hansen, D. O'Hare, *J. Am. Chem. Soc.* **2001**, *123*, 12547 – 12555; e) A. G. Whittaker, A. Harrison, G. S. Oakley, I. D. Youngson, R. K. Heenan, S. M. King, *Rev. Sci. Instrum.* **2001**, *72*, 173 – 176.

[40] a) J. Weidlein, U. Müller, K. Dehnicke in *Schwingungsspektroskopie*, Thieme, Stuttgart, **1988**; b) P. W. Atkins in *Quanten*, VCH, Weinheim, **1993**; c) B. Schrader in *Infrared and Raman Spectroscopy*, VCH, Weinheim, **1995**.

[41] G. Fevotte, *Trans. IChemE Part A* **2007**, *85*, 906 – 920.

[42] a) G. J. Vergote, C. Vervaet, J. P. Remon, T. Haemers, F. Verpoort, *Eur. J. Pharm. Sci.* **2002**, *16*, 63 – 67; b) S. Wartewig, R. H. H. Neubert, *Adv. Drug Delivery Rev.* **2005**, *57*, 1144 – 1170.

[43] a) T. Okumura, M. Matsuoka, *Pharm. Res.* **2005**, *22*, 1350 – 1357; b) V. P. Lehto, M. Tenho, K. Vaha-Heikkila, P. Harjunen, M. Paallysaho, J. Valisaari, P. Niemela, K. Jarvinen, *Powder Technol.* **2006**, *167*, 85 – 93.

[44] a) D. Pratiwi, J. P. Fawcett, K. C. Gordon, T. Rades, *Eur. J. Pharm. Biopharm.* **2002**, *54*, 337 – 341; b) M. E. Auer, U. J. Griesser, J. Sawatzki, *J. Mol. Struct.* **2003**, *661–662*, 307 – 317; c) Z. Német, B. Hegedus, C. Szantay, Jr., J. Sztatisz, G. Pokol, *Thermochim. Acta* **2005**, *430*, 35 – 41.

[45] E. Boccaleri, F. Carniato, G. Croce, D. Viterbo, W. van Beek, H. Emerich, M. Milanesio, *J. Appl. Crystallogr.* **2007**, *40*, 684 – 693.

[46] F. Fan, Z. Feng, G. Li, K. Sun, P. Ying, C. Li, *Chem. Eur. J.* **2008**, *14*, 5125 – 5129.

[47] M. G. O'Brien, A. M. Beale, R. A. Catlow, B. M. Weckhuysen, *J. Am. Chem. Soc.* **2006**, *128*, 11744 – 11745.

[48] H. Taniguchi, J. Yu, Y. Arai, T. Yagi, D. Fu, M. Itoh, *Ferroelectrics* **2007**, *346*, 156 – 161.

[49] N. Sugita, E. Tokumitsu, M. Osada, M. Kakihana, *Jpn. J. Appl. Phys.* **2003**, *42*, L944 – L945.

[50] http://las.perkinelmer.com/content/technicalinfo/tch_ftiratr.pdf.

[51] a) J. Cornel, C. Lindenberg, M. Mazzotti, *Ind. Eng. Chem. Res.* **2008**, *47*, 4870 – 4882; b) J. Thun, L. Seyfarth, J. Senker, R. E. Dinnebier, J. Breu, *Angew. Chem.* **2007**, *119*, 6851 – 6854; *Angew. Chem. Int. Ed.* **2007**, *46*, 6729 – 6731.

[52] a) H. Budzikiewicz, M. Schäfer in *Massenspektrometrie, eine Einführung*, 5th ed., Wiley-VCH, Weinheim, **2005**; b) J. H. Gross in *Mass Spectrometry*, Springer, Berlin, **2004**.

[53] a) P. Bussian, F. Sobott, B. Brutschy, W. Schrader, F. Schüth, *Angew. Chem.* **2000**, *112*, 4065 – 4069; *Angew. Chem. Int. Ed.* **2000**, *39*, 3901 – 3905; b) S. A. Pelster, W. Schrader, F. Schüth, *J. Am. Chem. Soc.* **2006**, *128*, 4310 – 4317; c) S. A. Pelster, R. Kalamajka, W. Schrader, F. Schüth, *Angew. Chem.* **2007**, *119*, 2349 – 2352; *Angew. Chem. Int. Ed.* **2007**, *46*, 2299 – 2302; d) S. A. Pelster, B. Weimann, B. B. Schaack, W. Schrader, F. Schüth, *Angew. Chem.* **2007**, *119*, 6794 – 6797; *Angew. Chem. Int. Ed.* **2007**, *46*, 6674 – 6677; e) B. B. Schaack, W. Schrader, F. Schüth, *Angew. Chem.* **2008**, *120*, 9232 – 9235; *Angew. Chem. Int. Ed.* **2008**, *47*, 9092 – 9095.

[54] a) M. Dole, L. L. Mack, R. L. Hines, R. C. Mobley, L. D. Ferguson, M. B. Alice, *J. Chem. Phys.* **1968**, *49*, 2240 – 2249; b) M. Yamashita, J. B. Fenn, *J. Phys. Chem.* **1984**, *88*, 4671 – 4675.

[55] W. Schilling, L. K. Thomas in *Bergmann, Schaefer, Lehrbuch der Experimentalphysik, Band 6 Festkörper*, 2nd ed. (Ed.: R. Kassing), de Gruyter, Berlin, **2005**.

[56] a) W. Blum, D. Hesse, *Solid State Ionics* **1997**, *95*, 41 – 49; b) D. Hesse, J. Heydenreich, *Fresenius J. Anal. Chem.* **1994**, *349*, 117 – 121; c) V. Teodorescu, L. Nistor, H. Bender, A. Steegen, A. Lauwers, K. Maex, J. Van Landuyt, *J. Appl. Phys.* **2001**, *90*, 167 – 174; d) T. Tanigaki, K. Ito, Y. Nagakubo, T. Asakawa, T. Kanemura, *J. Electron Microsc.* **2009**, *58*, 281 – 287; e) S.-Y. Chung, Y.-M. Kim, J.-G. Kim, Y.-J. Kim, *Nat. Phys.* **2009**, *5*, 68 – 73; f) J. M. Howe, H. Saka, *MRS Bull.* **2004**, *29*, 951 – 957; g) P. W. Sutter, E. A. Sutter, *Nat. Mater.* **2007**, *6*, 363 – 366.

[57] a) C. N. Banwell, E. M. McCash in *Molekülspektroskopie*, Oldenbourg, Munich, **1999**; b) J. Senker, J. Sehnert, S. Correll, *J. Am. Chem. Soc.* **2005**, *127*, 337 – 349.

[58] O. B. Vistad, D. E. Akporiaye, F. Taulelle, K. P. Lillerud, *Chem. Mater.* **2003**, *15*, 1639 – 1649.

[59] a) J. Shi, M. W. Anderson, S. W. Carr, *Chem. Mater.* **1996**, *8*, 369 – 375; b) Z. Miladinovic, J. Zakrzewska, B. Kovacevi, G. Bacic, *Mater. Chem. Phys.* **2007**, *104*, 384 – 389.

[60] M. Haouas, C. Gerardin, F. Taulelle, C. Estournes, T. Loiseau, G. Ferey, *J. Chim. Phys.* **1998**, *95*, 302 – 309.

[61] F. Taulelle, M. Haouas, C. Gerardin, C. Estournes, T. Loiseau, G. Ferey, *Colloids Surf. A* **1999**, *158*, 299 – 311.

[62] H. Liu, H. Ernst, D. Freude, F. Scheffler, W. Schwieger, *Microporous Mesoporous Mater.* **2002**, *54*, 319 – 330.

[63] C. E. Hughes, K. D. M. Harris, *J. Phys. Chem. A* **2008**, *112*, 6808 – 6810.

[64] a) D. Grandjean, A. M. Beale, A. V. Petukhov, B. M. Weckhuysen, *J. Am. Chem. Soc.* **2005**, *127*, 14454 – 14465; b) R. A. van Santen, *Nature* **2006**, *444*, 46 – 47; c) K. Simmance, G. Sankar, R. G. Bell, C. Prestipino, W. van Beek, *Phys. Chem. Chem. Phys.* **2010**, *12*, 559 – 562; d) A. M. Beale, G. Sankar, *Nucl.*

Instrum. Methods Phys. Res. Sect. B **2003**, *199*, 504 – 508; e) A. M. Beale, L. M. Reilly, G. Sankar, *Appl. Catal. A* **2007**, *325*, 290 – 295; f) W. Fan, M. Ogura, G. Sankar, T. Okubo, *Chem. Mater.* **2007**, *19*, 1906 – 1917; g) C. Aletru, G. N. Greaves, G. Sankar, *J. Phys. Chem. B* **1999**, *103*, 4147 – 4152; h) G. Sankar, W. Bras, *Catal. Today* **2009**, *145*, 195 – 203.

[65] H. Putz, J. C. Schön, M. Jansen, *Comput. Mater. Sci.* **1998**, *11*, 309 – 322.

[66] a) Y. Liebold-Ribeiro, D. Fischer, M. Jansen, *Angew. Chem.* **2008**, *120*, 4500 – 4503; *Angew. Chem. Int. Ed.* **2008**, *47*, 4428 – 4431; b) A. R. Oganov, C. W. Glass, S. Ono, *Earth Planet. Sci. Lett.* **2006**, *241*, 95 – 103.

[67] a) J. C. Schön, Z. Cancarevic, M. Jansen, *J. Chem. Phys.* **2004**, *121*, 2289 – 2304; b) Z. Cancarevic, J. C. Schön, M. Jansen, *Phys. Rev. B* **2006**, *73*, 224114; c) K. Doll, J. C. Schön, M. Jansen, *Phys. Chem. Chem. Phys.* **2007**, *9*, 6128 – 6133; d) Z. P. Cancarevic, J. C. Schön, M. Jansen, *Chem. Asian J.* **2008**, *3*, 561 – 572; e) K. Doll, J. C. Schön, M. Jansen, *Phys. Rev. B* **2008**, *78*, 144110; f) J. C. Schön, M. Jansen, *Int. J. Mater. Res.* **2009**, *100*, 135 – 146; g) A. R. Oganov, M. Valle, *J. Chem. Phys.* **2009**, *130*, 104504 – 104509; h) J. C. Schön, K. Doll, M. Jansen, *Phys. Status Solidi B* **2010**, *247*, 23 – 39.

[68] a) C. Mellot-Draznieks, J. M. Newsam, A. G. Gorman, C. M. Freeman, G. Férey, *Angew. Chem.* **2000**, *112*, 2358 – 2363; *Angew. Chem. Int. Ed.* **2000**, *39*, 2270 – 2275; b) C. Mellot-Draznieks, S. Girard, G. Férey, J. C. Schön, Z. Cancarevic, M. Jansen, *Chem. Eur. J.* **2002**, *8*, 4102 – 4113; c) C. Mellot-Draznieks, S. Girard, G. Férey, *J. Am. Chem. Soc.* **2002**, *124*, 15326 – 15335; d) C. Mellot-Draznieks, J. Dutour, G. Férey, *Angew. Chem.* **2004**, *116*, 6450 – 6456; *Angew. Chem. Int. Ed.* **2004**, *43*, 6290 – 6296.

[69] a) P. Raiteri, R. Martonak, M. Parrinello, *Angew. Chem.* **2005**, *117*, 3835 – 3839; *Angew. Chem. Int. Ed.* **2005**, *44*, 3769 – 3773; b) A. R. Oganov, C. W. Glass, *J. Chem. Phys.* **2006**, *124*, 244704; c) C. W. Glass, A. R. Oganov, N. Hansen, *Comput. Phys. Commun.* **2006**, *175*, 713 – 720; d) D. Zahn, *J. Phys. Chem. B* **2007**, *111*, 5249 – 5253; e) A. Kawska, P. Duchstein, O. Hochrein, D. Zahn, *Nano Lett.* **2008**, *8*, 2336 – 2340; f) M. A. Neumann, F. J. J. Leusen, J. Kendrick, *Angew. Chem.* **2008**, *120*, 2461 – 2464; *Angew. Chem. Int. Ed.* **2008**, *47*, 2427 – 2430; g) A. Kawska, O. Hochrein, J. Brickmann, R. Kniep, D. Zahn, *Angew. Chem.* **2008**, *120*, 5060 – 5063; *Angew. Chem. Int. Ed.* **2008**, *47*, 4982 – 4985; h) S. M. Woodley, R. Catlow, *Nat. Mater.* **2008**, *7*, 937 – 946.

[70] G. Chkonia, J. Wölk, R. Strey, J. Wedekind, D. Reguera, *J. Chem. Phys.* **2009**, *130*, 064505.

[71] J. Wedekind, R. Strey, D. Reguera, *J. Chem. Phys.* **2007**, *126*, 134103.

[72] F. Schüth, *Curr. Opin. Solid State Mater. Sci.* **2001**, *5*, 389 – 395.

[73] J. Anwar, D. Zahn, *Angew. Chem.* **2011**, 123, DOI: 10.1002/ange.201000463; *Angew. Chem. Int. Ed.* **2011**, *50*, DOI: 10.1002/anie.201000463.

[74] a) W. S. Sheldrick, M. Wachhold, *Angew. Chem.* **1997**, *109*, 214 – 234; *Angew. Chem. Int. Ed. Engl.* **1997**, *36*, 206 – 224; b) W. S. Sheldrick, M. Wachhold, *Coord. Chem. Rev.* **1998**, *176*, 211 – 322; c) W. S. Sheldrick, *J. Chem. Soc. Dalton Trans.* **2000**, 3041 – 3052; d) X. Bu, N. Zheng, P. Feng, *Chem. Eur. J.* **2004**, *10*, 3356 – 3362; e) P. Feng, X. Bu, N. Zheng, *Acc. Chem. Res.* **2005**, *38*, 293 – 303; f) M. G. Kanatzidis, *Adv. Mater.* **2007**, *19*, 1165 – 1181; g) S. Dehnen, M. Melullis, *Coord. Chem. Rev.* **2007**, *251*, 1259 – 1280; h) Q. Zhang, X. Bu, Z. Lin, T. Wu, P. Feng, *Inorg. Chem.* **2008**, *47*, 9724 – 9726; i) J. Zhou, J. Dai, G.-Q. Bian, C.-Y. Li, *Coord. Chem. Rev.* **2009**, *253*, 1221 – 1247.

[75] a) M. T. Pope, A. Müller, *Angew. Chem.* **1991**, *103*, 56 – 70; *Angew. Chem. Int. Ed. Engl.* **1991**, *30*, 34 – 48; b) D. E. Katsoulis, *Chem. Rev.* **1998**, *98*, 359 – 387; c) A. Müller, P. Kögerler, *Coord. Chem. Rev.* **1999**, *182*, 3 – 17; d) A. Müller, P. Kögerler, C. Kuhlmann, *Chem. Commun.* **1999**, 1347 – 1358; e) L. Cronin, P. Kögerler, A. Müller, *J. Solid State Chem.* **2000**, *152*, 57 – 67; f) C.-D. Zhang, S.-X. Liu, B. Gao, C.-Y. Sun, L.-H. Xie, M. Yu, J. Peng, *Polyhedron* **2007**, *26*, 1514 – 1522; g) A. Proust, R. Thouvenot, P. Gouzerh, *Chem. Commun.* **2008**, 1837 – 1852.

[76] a) G. Demazeau, *J. Mater. Chem.* **1999**, *9*, 15 – 18; b) R. I. Walton, *Chem. Soc. Rev.* **2002**, *31*, 230 – 238; c) R. E. Riman, W. L. Suchanek, M. M. Lencka, *Ann. Chem. Sci. Mater.* **2002**, *27*, 15 – 36; d) J. O. Eckert, C. C. Hung-Houston, B. L. Gersten, M. M. Lencka, R. E. Riman, *J. Am. Ceram. Soc.* **1996**, *79*, 2929 – 2939; e) J. Spooren, A. Rumplecker, F. Millange, R. I. Walton, *Chem. Mater.* **2003**, *15*, 1401 – 1403; f) J. J. Urban, L. Ouyang, M. H. Jo, D. S. Wang, H. Park, *Nano Lett.* **2004**, *4*, 1547 – 1550; g) C. Chen, J. R. Cheng, S. W. Yu, L. J. Che, Z. Y. Meng, *J. Cryst. Growth* **2006**, *291*, 135 – 139.

[77] R. Francis, D. O'Hare, *J. Chem. Soc. Dalton Trans.* **1998**, 3133 – 3148.

[78] P. Barnes, S. M. Clark, C. H. Fentiman, D. Häusermann, E. Henderson, M. N. Muhamad, S. Rashid, *Phase Transitions* **1991**, *39*, 117 – 128.

[79] M. D. Maeder, D. Damjanovic, N. Setter, *J. Electroceram.* **2004**, *13*, 385 – 392.

[80] a) I. Santos, L. H. Loureiro, M. F. P. Silva, A. M. V. Cavaleiro, *Polyhedron* **2002**, *21*, 2009 – 2015; b) G. K. L. Goh, F. L. Lange, S. M. Haile, C. G. Levi, *J. Mater. Res.* **2003**, *18*, 338 – 345; c) H. Y. Zhu, Z. F. Zheng, X. P. Gao, Y. N. Huang, Z. M. Yan, J. Zou, H. M. Yin, Q. D. Zou, S. H. Kable, J. C. Zhao, Y. F. Xi, W. N. Martens, R. L. Frost, *J. Am. Chem. Soc.* **2006**, *128*, 2373 – 2384; d) A. J. Paula, M. A. Zaghete, E. Longo, J. A. Varela, *Eur. J. Inorg. Chem.* **2008**, 1300 – 1308.

[81] A. M. Beale, A. M. J. van der Eerden, S. D. M. Jacques, O. Leynaud, M. G. O'Brien, F. Meneau, S. Nikitenko, W. Bras, B. M. Weckhuysen, *J. Am. Chem. Soc.* **2006**, *128*, 12386 – 12387.

[82] a) P. Bussian, W. Schmidt, F. Schüth, P. Ågren, J. Andersson, M. Lindén, H. Amenitsch in *ELETTRA Highlights (Research Highlights)* (Eds.: M. Altarelli, C. J. Bocchetta, K. D. Carugo, A. Goldoni, C. Grubissa, W. Jark, M. Matteucci, R. P. Walker), ELETTRA, Triest (http://www.elettra.trieste.it/science/highlights), **2000–2001**, pp. 30 – 32; b) W. Schmidt, P. Bussian, M. Lindén, H. Amenitsch, P. Ågren, M. Tiemann, F. Schüth, *J. Am. Chem. Soc.* **2010**, *132*, 6822 – 6826; c) M. Tiemann, Ö. Weiß, J. Hartikainen, F. Marlow, M. Linden, *ChemPhysChem* **2005**, *6*, 2113 – 2119; d) M. Tiemann, F. Marlow, F. Brieler, M. Linden, *J. Phys. Chem. B* **2006**, *110*, 23142 – 23147; e) M. Tiemann, F. Marlow, J. Hartikainen, Ö. Weiß, M. Linden, *J. Phys. Chem. C* **2008**, *112*, 1463 – 1467.

[83] T. Barnardo, K. Hoydalsvik, R. Winter, C. M. Martin, G. F. Clark, *J. Phys. Chem. C* **2009**, *113*, 10021 – 10028.

[84] J. Brendt, D. Samuelis, T. E. Weirich, M. Martin, *Phys. Chem. Chem. Phys.* **2009**, *11*, 3127 – 3137.

[85] a) S. Ekambaram, *J. Alloys Compd.* **2005**, *390*, L4 – 6; b) T. Sritharan, S. Murali, *J. Mater. Process. Technol.* **2001**, *113*, 469 – 473; c) M. A. Rodriguez, N. S. Makhonin, J. A. Escrina, I. P. Borovinskaya, M. I. Osendi, M. F. Barba, J. E. Iglesias, J. S. Moya, *Adv. Mater.* **1995**, *7*, 745 – 747; d) J. S. Moya, J. E. Iglesias, J. Limpo, J. A. Escrina, N. S. Makhonin, M. A. Rodriguez, *Acta Mater.* **1997**, *45*, 3089 – 3094; e) M. A. Rodríguez, F. J. Limpo, J. A. Escrina, N. S. Makhonin, M. I. Osendi, M. F. Barba, J. E. Iglesias, J. S. Moya, *Scr. Mater.* **1997**, *37*, 405 – 410; f) A. K. Khanra, L. C. Pathak, S. K. Mishra, M. M. Godkhindi, *Mater. Lett.* **2004**, *58*, 733 – 738.

[86] C. Curfs, X. Turillas, G. B. M. Vaughan, A. E. Terry, A. Kvick, M. A. Rodriguez, *Intermetallics* **2007**, *15*, 1163 – 1171.

[87] J. G. Mesu, A. M. J. van der Eerden, F. M. F. de Groot, B. M. Weckhuysen, *J. Phys. Chem. B* **2005**, *109*, 4042 – 4047.

[88] a) V. Briois, D. Lützenkirchen-Hecht, F. Villain, E. Fonda, S. Belin, B. Griesebock, R. Frahm, *J. Phys. Chem. A* **2005**, *109*, 320 – 329; b) E. de Smit, I. Swart, J. F. Creemer, G. H. Hoveling,

M. K. Gilles, T. Tyliszczak, P. J. Kooyman, H. W. Zandbergen, C. Morin, B. M. Weckhuysen, F. M. F. de Groot, *Nature* **2008**, *456*, 222 – 226; c) J. Evans, M. Tromp, *J. Phys. Condens. Matter* **2008**, *20*, 184020 – 184029; d) D. Ferri, A. Baiker, *Top. Catal.* **2009**, *52*, 1323 – 1333.

[89] a) L. O. Martinez Tomalino, W. Peukert, *Nachr. Chem.* **2008**, *56*, 551 – 554; b) L. Schneider, W. Peukert, *Part. Part. Syst. Charact.* **2006**, *23*, 351 – 359; c) L. Schneider, H. J. Schmidt, W. Peukert, *Appl. Phys. B* **2007**, *87*, 333 – 339; d) B. Schürer, D. Segets, L. Martinez Tomalino, W. Peukert, *Chem. Ing. Tech.* **2008**, *80*, 1410 – 1411.

[90] L. Martinez Tomalino, A. Voronov, A. Kohut, W. Peukert, *J. Phys. Chem. B* **2008**, *112*, 6338 – 6343.

[91] D. Segets, L. M. Tomalino, J. Gradl, W. Peukert, *J. Phys. Chem. C* **2009**, *113*, 11995 – 12001.

[92] D. Segets, J. Gradl, R. K. Taylor, V. Vassilev, W. Peukert, *ACS Nano* **2009**, *3*, 1703 – 1710.

[93] a) S. J. L. Billinge, *J. Solid State Chem.* **2008**, *181*, 1695 – 1700; b) T. Proffen, H. Kim, *J. Mater. Chem.* **2009**, *19*, 5078 – 5088; c) V. Petkov, *Mater. Today* **2008**, *11*, 28 – 38.

